

Financial modeling of climate risk supports stringent mitigation action

Adam Michael Bauer*

Cristian Proistosescu†

Gernot Wagner‡

Working Paper

February 7, 2023

Abstract

Valuing the cost of carbon dioxide (CO_2) emissions is vital in weighing viable approaches to climate policy. Conventional approaches to pricing CO_2 evaluate trade-offs between sacrificing consumption now to abate CO_2 emissions versus growing the economy, therefore enlarging one's financial resources to pay for climate damages later, all within a standard Ramsey growth framework. However, these approaches fail to comprehensively incorporate decision making under risk and uncertainty in their analysis, a limitation especially relevant considering the tail risks of climate impacts. Here, we take a financial-economic approach to carbon pricing by developing the Carbon Asset Pricing model – AR6 (CAP6), which prices CO_2 emissions as an asset with negative returns and allows for an explicit representation of risk in its model structure. CAP6's emissions projections, climate damage functions, climate emulator, and mitigation cost function are in line with the sixth assessment report (AR6) from the Intergovernmental Panel on Climate Change (IPCC). The economic parameters (such as the discount rate) are calibrated to reflect recent empirical work.

We find that in our main specification, CAP6 provides support for a high carbon price in the near-term that declines over time, with a resulting ‘optimal’ expected warming below the 1.5 °C target set forth in the Paris agreement. We find that, even if the cost of mitigating CO_2 emissions is much higher than what is estimated by the IPCC, CAP6 still provides support for a high carbon price, and the resulting ‘optimal’ warming stays below 2 °C (albeit warming does exceed 1.5 °C by 2100). Incorporating learning by doing further lowers expected warming while making ‘optimal’ policy more cost effective. By decomposing sources of climate damages, we find that risk associated with slowed economic growth has an outsized influence on climate risk assessment in comparison to static-in-time estimates of climate damages.

In a sensitivity analysis, we sample a range of discount rates and technological growth rates, and disentangle the role of each of these assumptions in determining central estimates of CAP6 output as well as its uncertainty over time. We find that central estimates of carbon prices are sensitive to assumptions around emissions projections, whereas estimates of warming, CO_2 concentrations, and economic damages are largely robust to such assumptions. We decompose the uncertainty in CO_2 prices, temperature rise, atmospheric CO_2 levels, and economic damages over time, finding that

*Department of Physics, University of Illinois at Urbana Champaign, Loomis Laboratory, Urbana, IL 61801 (corresponding author: adammb4@illinois.edu)

†Department of Atmospheric Sciences & Department of Geology, University of Illinois at Urbana Champaign, Urbana, IL 61801 (cristi@illinois.edu)

‡Columbia Business School, New York, NY 10027 (gwagner@columbia.edu)

individual preferences control price uncertainty in the near term, while rates of technological change drive price uncertainty in the distant future. The influence of individual preferences on temperature rise, CO₂ concentrations, and economic damages is realized for longer than in the case of CO₂ prices owing to the consequences of early inaction. Taken in totality, our work highlights the necessity of early and stringent action to mitigate CO₂ emissions in addressing the dangers posed by climate change.

Contents

1	Introduction	4
2	Model framework	6
2.1	Socio-economic framework	6
2.1.1	Economic utility	7
2.1.2	Emission baselines	10
2.1.3	Damage functions	11
2.1.4	Cost of mitigation	16
2.2	Climate model	21
2.2.1	Mapping emissions to temperature anomaly above preindustrial	21
2.2.2	Carbon cycle model	22
2.3	Prototypical model run	23
2.4	Model calibration	25
2.4.1	Preferred and featured runs	26
2.4.2	Ensemble runs	26
3	Results	27
3.1	Main specification	27
3.1.1	Isolating sources of climate-economic risk	29
3.2	Alternative calibrations	30
3.2.1	“No free lunches” calibration	30
3.2.2	“Learning by doing” demonstration	32
3.3	Ensemble model analysis	32
3.3.1	Variance decomposition of ensemble results	34
4	Discussion	36
4.1	Key findings	36
4.2	Limitations and directions for future work	38

A Damage function calibration

39

B Regression analysis

40

1 Introduction

CLIMATE change’s impact on the economy first gained prominence in the economics literature some 30 years ago, when the first climate-economic Integrated Assessment Model (IAM) calculated the cost of a marginal ton of carbon dioxide (CO_2) emissions to society, coined the ‘Social Cost of Carbon’ (SCC) [76]. Since this breakthrough in climate-economic modeling, IAMs have taken center stage in the climate policy discussion, with the resulting SCC projections being utilized by numerous companies, government bodies, and agencies worldwide [105]. Conventional IAMs (such as the dynamic integrated climate-economy, or DICE [76, 77, 78]) evaluate climate change impacts within the context of a standard Ramsey growth economy. In this approach, one considers tradeoffs between emitting CO_2 and incurring damages both now and, largely, in the future, versus abating CO_2 emissions now for some cost. The resulting benefit-cost analysis results in a presently-low ($\sim \$40$ in the case of DICE–2016R [78]) and rising ‘optimal’ price over time, with significant warming ($\sim 4^\circ\text{C}$) by 2100. A recent IAM – the Greenhouse gas Impact Value Evaluator (GIVE) – that employs this framework found a much larger present-day SCC of \$185 [83] (an increase from the United States Interagency Working Group central estimate of \$51 [14] and in line with the United States Environmental Protection Agency’s recent estimates [72]), but did not explore the optimal control problem of weighing the benefits and costs of abating CO_2 emissions, instead focusing on the marginal damage associated with each ton of CO_2 emitted. It is notable that DICE’s suggested ‘optimal’ warming projections are larger than the warming target of 1.5°C established in the Paris Agreement [98]. While this inconsistency has called into question the authority of such models in the climate policy discussion to some [80, 93], DICE can be made consistent with a warming target of 1.5°C with alternative damages and discount rate assumptions [33].

A limitation of Ramsey growth IAMs is that they lack a comprehensive description of decision-making under uncertainty, a feature of many financial economics models [16, 2, 6]. This is important, as climate change projections are inherently probabilistic, with low probability, extreme impact outcomes presenting the most significant risk to the climate-economic system (i.e., a potentially high climate response to emissions leading to rapid warming). Additionally, many complex risks associated with climate change cannot currently be fully quantified and are therefore excluded from economic analyses, despite impacting the overall risk landscape of climate impacts [87]. An example of this are climate tipping points, which have been argued to lead to rapid environmental degradation [61, 5] and increase the SCC [20]. These “deep” uncertainties in the impacts of climate change have led some to advocate for an “insurance” to be taken out against high climate damages [104]. Ramsey growth models do not allow for such considerations in determining their policy projections. Put differently: Ramsey growth IAMs do not allow individuals to ‘hedge’ against climate catastrophe.

Recently, financial asset pricing models have been introduced in an effort to understand how risk impacts climate policy decision making [18, 19, 10]. Such models take a fundamentally different approach than conventional, Ramsey growth IAMs. Instead of computing the “shadow price” of CO_2 (which is to say, the price of CO_2 implied from distortions in consumption and economic utility owing to climate damages), financial asset pricing models compute the price of CO_2 directly, treating CO_2 as an asset with negative returns. The result is not the SCC of yore, but rather, a direct ‘optimal’ price for each ton of CO_2 emitted. However, implementations of such models have lacked accurate representations

of the climate system, utilized *ad hoc* parameterizations of climate tipping points and their associated damages, and implemented a climate damage function that does not align with recent literature.

Here, we introduce the Carbon Asset Pricing model – AR6 (abbreviated to CAP6 herein), a climate-economy IAM that builds on previous financial asset pricing climate-economy models [18, 19]. CAP6 embeds a representative agent in a binomial, path dependent tree that models decision making under uncertainty. Prior to optimization, a number of potential trees are generated via sampling climate and climate impacts uncertainty that the agent traverses depending on emissions abatement choices. The present-day Epstein-Zin (EZ) utility of consumption [23, 103, 24] is optimized to determine the ‘optimal’ emissions abatement policy. EZ utility allows for the separation of risk aversion across states of time and states of nature, a distinction theorized to play a significant role in climate policy [2, 60].

CAP6 is a fully modular IAM, with up-to-date estimates for the exogenous emissions baselines, climate response to emissions, climate damage functions, and abatement costs consistent with the sixth assessment report (AR6) issued by the Intergovernmental Panel on Climate Change (IPCC) [42, 43, 44]. We take the shared socio-economic pathways (SSPs) as our exogenous emissions baselines [100, 25, 26, 11, 56, 85]. The climate component of the model utilizes an effective transient climate response to emissions (TCRE) to map cumulative emissions to global mean surface temperature (GMST) anomaly [4, 62, 21, 17, 42], and a simple carbon cycle model to map CO₂ emissions to concentrations [51]. We sample with equal probability three damage functions of different shape and scale [8, 89, 95, 41], thus capturing both parametric and epistemic uncertainty in the damage function in our risk assessment. Finally, we formulate a new marginal abatement cost curve (MACC), providing a much-needed update to the McKinsey MACC [66, 29].

We present our findings in two parts. The first is a set of calibrations that are in line with the recent literature (i.e., empirically calibrated discount rates [99, 75]) and showcase the influence of different assumptions on model output. In each of these calibrations, we find that the carbon price is high in the near term and declines over time, providing support for stringent mitigation action. Most notably, we find that the ‘optimal’ expected warming in the preferred calibration is in line with the 1.5 °C of warming by 2100 target set forth in the Paris agreement. Furthermore, we find that even if we are pessimistic about the cost estimates provided by the IPCC, the preferred calibration of CAP6 still supports limiting warming to less than 2 °C warming by 2100. We demonstrate the role of learning by doing by allowing for endogenous technological growth, and find that this decreases the overall costs of ‘optimal’ policy and lowers expected warming. We show that risk associated with slowing economic growth has an outsized influence on price path dynamics in comparison to static-in-time estimates of climate damages, and argue this is a general feature of CAP6 ‘optimal’ price paths.

The second presentation of model results is in a sensitivity analysis where we randomly sample a set of discount rates, risk aversion levels, and technological growth rates. We show that while the expected carbon price depends on the emissions baseline, the expected temperature rise, level of CO₂ concentrations, and incurred economic damages is not. This suggests that our model robustly calculates an economically ‘optimal’ temperature level; the price of actualizing this temperature level varies across baselines owing to assumptions about how much emissions are decreasing independently of the policy implemented in CAP6. We find that price uncertainty is dominated by discounting in the near-term and the technological growth rate in the far-term. On the other hand, temperature rise, CO₂ concentration

level, and economic damage uncertainty are dominated by discounting for much longer than CO₂ prices, as early inaction leads to warming that cannot be undone later by spending more on abatement (in the absence of significant negative emissions or solar geoengineering).

The remainder of this paper is structured as follows. In § 2, we present the components of CAP6. The socio-economic framework is discussed in § 2.1; the climate module is introduced in § 2.2; and our calibration is presented in § 2.4. We present our results in § 3, and close with a discussion in § 4.

2 Model framework

THE cost of carbon and associated ‘optimal’ mitigation policy is computed by evaluating the trade-offs between environmental damage and economic growth. It is therefore natural to decompose our model exposition into a socio-economic component and a climate component. We discuss each of these in turn below, in § 2.1 and § 2.2, respectively. In each subsection, we provide a summary paragraph prior to the remaining technical details for those interested only in the key assumptions and equations in our model. We close this section with a statement of our utility optimization problem in § 2.1.1, an example of the mechanistic implementation of each of the CAP6 components into one complete model “run” in § 2.3, and a description of our model calibration in § 2.4.

2.1 Socio-economic framework

The socio-economic environment we describe here involves numerous assumptions about the world’s current state and how it will evolve in the future, such as: individual preferences towards risk and economic utility, decision making under uncertainty, projections of CO₂ emissions, the magnitude of climate change damages, and the cost of mitigating CO₂ emissions. Each of these are discussed in turn below.

A summary of our setup is as follows. We consider a representative agent with Epstein-Zin utility given by (2.1), and embed this individual in a binomial tree structure where their 2020 utility is optimized. See Figure 1 for a schematic of the tree structure. CO₂ emissions are projected under the shared socio-economic projections used by the IPCC (Figure 2). Climate damage functions are taken from the IPCC WGI results (with some important modifications to their statistically estimated damage function), and our uncertainty parameterization captures both epistemic and parametric uncertainty in the damage functions. The generic equation for our damage functions is given (2.6), with fitted parameter values and associated uncertainty summarized in Table 1. See Figure 6 for visualizations of each damage function. Finally, we employ (2.16) as our marginal abatement cost curve (Figure 4) and provide two calibrations: our ‘main specification’ based solely on the data in AR6, and the “no free lunches” calibration, which excludes negative costs in the AR6 cost data. Parameter values for each calibration of (2.16) are in Table 2.

2.1.1 Economic utility

CAP6 features the same economic setup as its predecessor [18, 19]. In contrast to Ramsey growth IAMs (such as DICE [78]), CAP6 considers a representative agent who maximizes their utility throughout time. In this way, CAP6 models how an *individual* would approach pricing CO₂; the output of CAP6 is then argued to be broadly true of society as a whole, hence the language of considering a “representative agent” of society. Broadly speaking, the societal welfare is an increasing function of the economic utility. Thus, by finding the maximum value of the economic utility, it is assumed that the society’s welfare is also maximized. We choose Epstein-Zin preferences [23, 24], described below, as our utility function because of its unique feature of separating risk across states of time and states of nature. This distinction has been theorized to be especially relevant for climate economic studies, where risk considerations across different dimensions, particularly related to extreme climatic events and tipping points, are important to consider [81, 20].

Epstein-Zin preferences

The discrete time utility, U_t , of a representative agent with Epstein-Zin (EZ) preferences [23, 24, 103] is given by

$$U_t = \left([1 - \beta]c_t^\rho + \beta [\mathbb{E}_t (U_{t+1}^\alpha)]^{\rho/\alpha} \right)^{1/\rho}, \quad (2.1)$$

where $\beta := (1 + \delta)^{-1} > 0$ and $\delta > 0$ is the pure rate of time preference (PRTP), $c_t > 0$ is the consumption at time t , $\rho := 1 - 1/\sigma$ and $\sigma > 0$ is the elasticity of intertemporal substitution (EIS), $\alpha := 1 - \psi$ and $\psi > 0$ is agent risk aversion (RA), and \mathbb{E}_t is the expectation operator at time t . When $\alpha = \rho$ (that is, when $\psi = 1/\sigma$), (2.1) collapses into the von Neumann-Morgenstern (VRM) expected utility index [101]. Assuming an exogenous growth rate of consumption $g > 0$, in the final period (occurring at time T), the utility is given by

$$U_T = \left[\frac{1 - \beta}{1 - \beta(1 + g)^\rho} \right]^{1/\rho} c_T. \quad (2.2)$$

Note that, in the EZ framework, risk aversion across time is parameterized by σ , whereas risk aversion across states of nature is parameterized by ψ . A larger value of either σ or ψ represents a higher degree of risk aversion along the respective dimension.

Tree structure

Agent utility in CAP6 is optimized within the structure of a binomial tree, therefore embedding the representative agent in a *finite horizon probability landscape*. This follows a standard approach employed in financial economics [16], and one useful to solve EZ-style models numerically [23, 24, 60].

The binomial tree structure of CAP6 is a representation of a time-evolving two dimensional probability distribution of climate damages (see Figure 1 for a schematic). The first dimension is time, while the second is “fragility”, the latter of which encodes the potential for high or low climate damages at a moment in time. Throughout, we will refer to the fragility coordinate at a time t as $\theta_t > 0$. Framing the

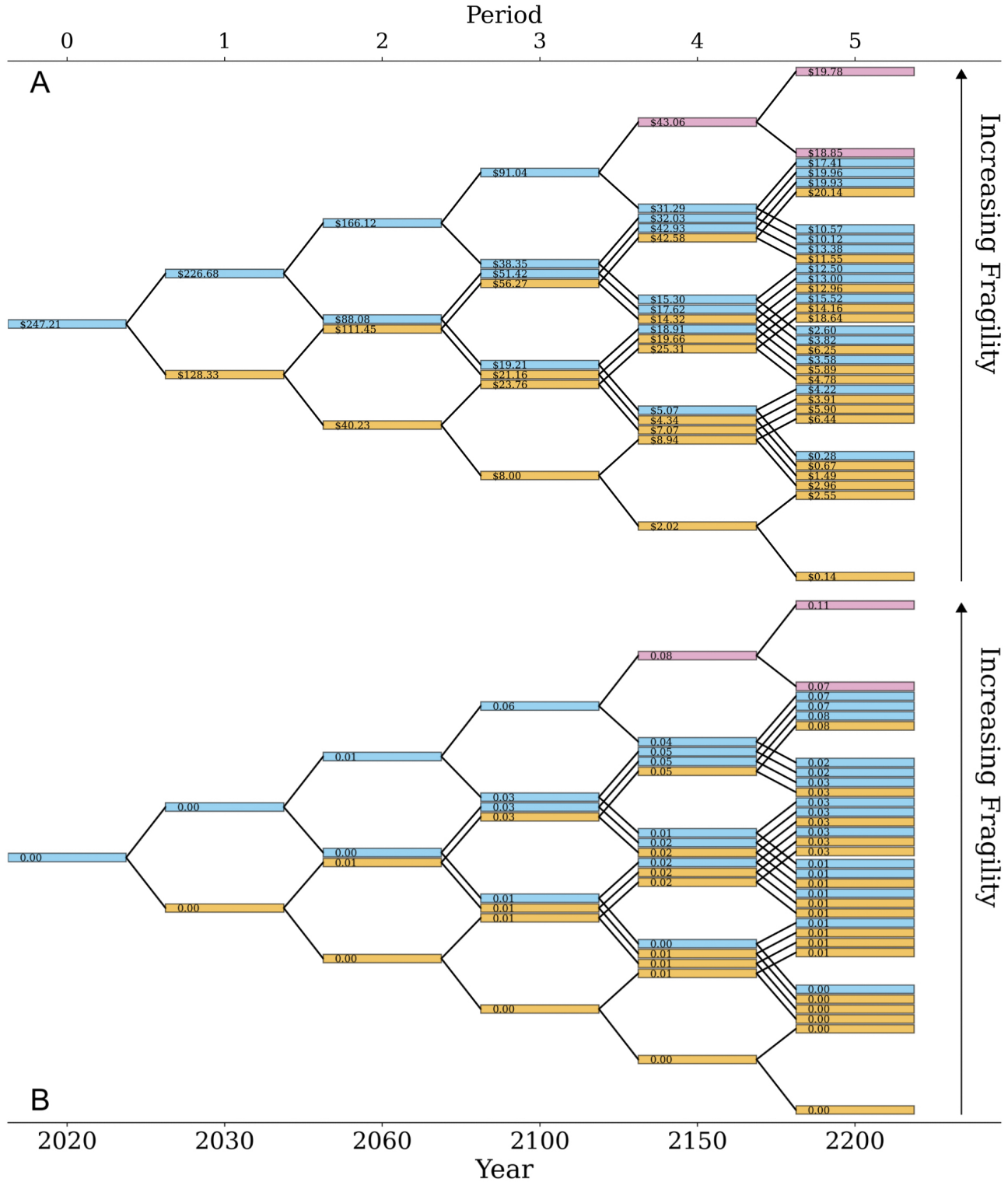


Figure 1: Binomial tree structure with CO₂ costs and climate damages. Panel **A** shows the cost of CO₂ at each node. Panel **B** shows the *agent experienced* climate damages at each node. Note that climate damages generally increase with fragility. In both panels, we highlight the accessible future states of two agents: one in 2150 (pink boxes) and one in 2030 (gold boxes). The values displayed are taken from our preferred model run.

tree structure as a representation of a two dimensional probability distribution allows for the roles of σ and ψ to be clarified: σ parameterizes risk aversion along the *time* dimension, while ψ parameterizes risk aversion along the “*fragility*” dimension. We choose to orient the fragility coordinate such that high (low, resp.) fragility is associated with high (low, resp.) climate damages. However, the origin of these high or low damages, both in the near and far term, is not explicitly represented. This owes to the fact that high climate damages could be owed to an unusually high climate response to emissions or a far-worse-than-imagined damage function, or both. The fragility parameter collapses all of these sources of uncertainty into a single parameter, based on a node’s position in the tree. By allowing for many agent decisions, and thus the generation of numerous nodes, we are able to coarsely represent the space of possible fragilities, therefore spanning many possible states of the climate and climate impacts, both in the near and far term. Note that in the limit of infinitely many decisions, fragility is normally distributed owing to every future state being equally likely, so as to not bias any outcome (be it sanguine or catastrophic) within the model structure.

Furthermore, this structure allows for uncertainty to directly influence agent decision making; as an example, consider two agents, one in 2150 and one in 2030 (see Figure 1). The agent in 2150 has only two future states accessible to her from her position in the tree; this represents an individual who knows well the impact of the climate on the economy. Compare this agent to another in 2030, who has a significantly higher number of future states accessible to him. This individual knows less about how climate change impacts the economy, which influences his decision making, as he has to weigh several possible futures with high and low climate damages all at once.

This choice of model structure, therefore, incorporates uncertainty directly into the decision making process as the individual optimizes their utility, rather than “abstracting from issues of uncertainty” [76] through post-facto, Monte-Carlo sampling of model inputs, as done in other studies (e.g., [14]). This approach fails to fully incorporate risk in its policy recommendations. Indeed, only recently has a fully probabilistic and self-consistent projection of the SCC been achieved within the Ramsey framework [83], but this study makes no claims in the direction of the “optimal control problem” of CO₂ emissions. In other words, it does not solve for the “optimal” control rate of CO₂ emissions, and only calculates the marginal damage of a ton of CO₂ emitted today.

Statement of utility optimization problem

Consider a representative agent embedded within a path-dependent binomial tree with T decision periods, leading to $2^T - 1$ total tree nodes. As the representative agent traverses the tree, she makes decisions so as to optimize her economic utility given by (2.1); in this way, the problem can be framed as a $2^T - 1$ dimensional optimization problem, as the utility is optimized at every node so as to maximize present-day utility.

The individual is placed within a standard endowment economy [94], where at every period time t she is given an amount \bar{c}_t . Note that $\bar{c}_t = \bar{c}_0(1 + g)^t$, and without loss of generality, we set \bar{c}_0 to unity. She cannot consume all of \bar{c}_t , however, owing to both climate change and climate policy. Climate change can cause the agent to lose some amount of \bar{c}_t due to climate damages, $\mathcal{D}_t \geq 0$. Climate policy impacts the individual’s consumption by allowing her to spend some amount of \bar{c}_t to reduce her impact on

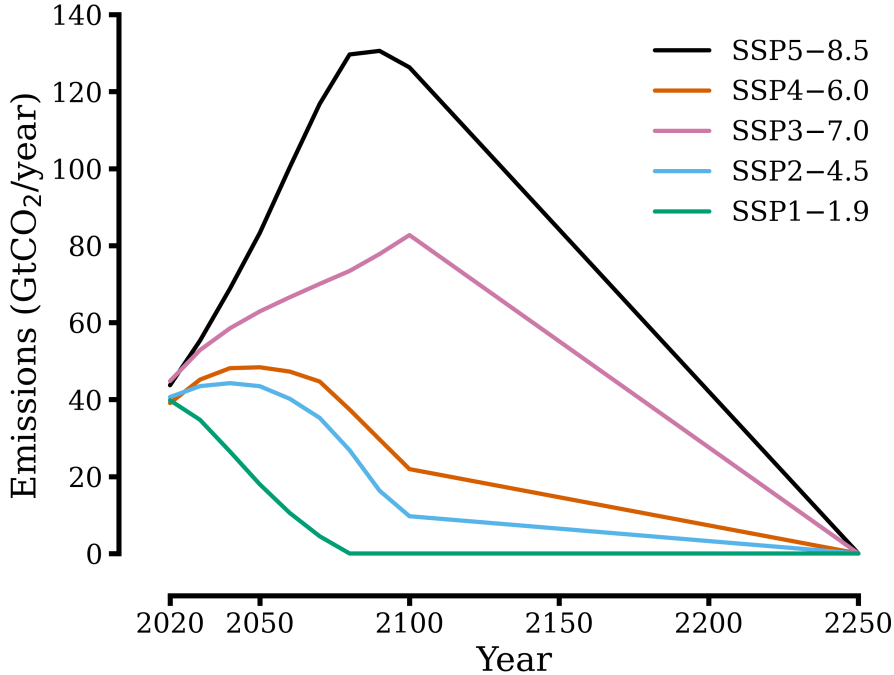


Figure 2: Emissions baselines. Shown are each of our emissions baselines with their extensions to 2250.

future climate by mitigating some fraction of emissions x_t ; the amount she chooses to spend is given by κ_t in (2.16). The consumption of the agent at each time $t \in \{0, 1, 2, \dots, T\}$ is thus determined by

$$c_0 = \bar{c}_0 (1 - \kappa_0(x_0)), \quad (2.3)$$

$$c_t = \bar{c}_t (1 - \kappa_t(x_t)) (1 - \mathcal{D}_t(\Psi_t, \theta_t, \mathcal{C}_t)), \quad \text{for } t \in \{1, 2, \dots, T-1\}, \quad (2.4)$$

$$c_T = \bar{c}_T (1 - \mathcal{D}_T(\Psi_T, \theta_T, \mathcal{C}_T)). \quad (2.5)$$

Given that the cost and cumulative emissions at a given time depend only on the mitigation vector, the problem of optimizing CAP6 boils down to finding the optimal mitigation vector x_t that maximizes the agent's economic utility at $t = 0$. We choose $T = 6$ decision periods in all the calculations in that follow, with our initial and final year being 2020 and 2250, respectively. While one may question the coarseness of our time discretization, it has been shown that including more decision periods in similar models does not significantly affect their output [13]. The remainder of this subsection will detail how climate damages and abatement costs are calculated.

2.1.2 Emission baselines

We use the standard set of shared socio-economic pathways (SSPs) [100, 25, 26, 11, 56, 85] as our exogenous CO₂ emission baselines, taking the emissions data for the period of 2020 – 2100 directly from the SSP database [27, 88], and span a range of end-of-century radiative forcing amounts. We make one alteration to the projections provided in the database: any negative emissions are set to zero. (This assumption only impacts SSP1–1.9, as SSP1–1.9 makes more optimistic assumptions around backstop technology than we do in our cost formulation, see § 2.1.4.) As our model extends out to 2250, we

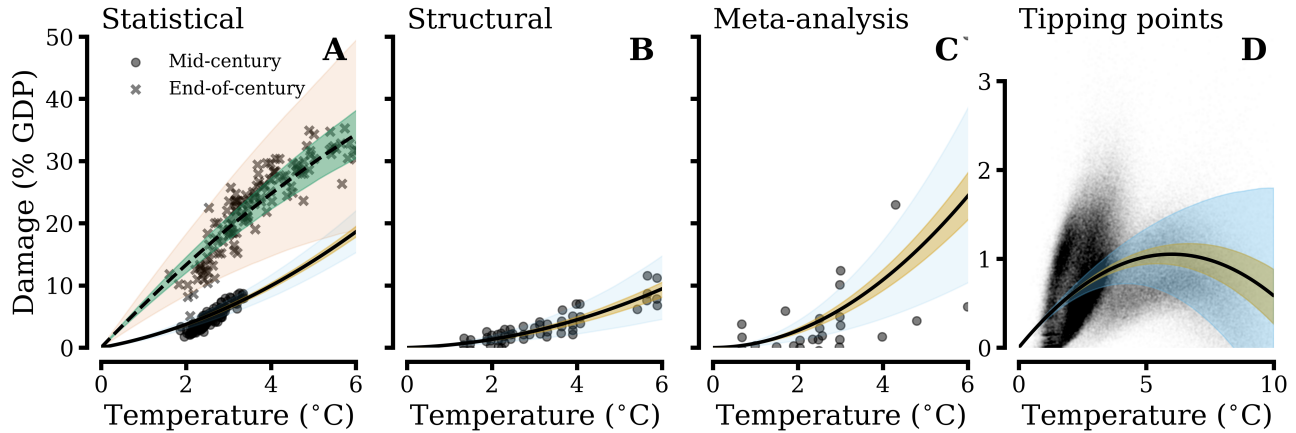


Figure 3: Damage functions. Shown are each of our damage functions by methodology (statistical, structural, and meta-analytic) as well as the marginal damages owing to tipping points. Note the statistical damage function shown assumes SSP2–4.5. In each panel, yellow shows ± 1 standard deviation in the damage function, while the blue shaded region shows ± 2 standard deviations. For the end of century estimates in panel A, the green region shown ± 1 standard deviation and the salmon shows ± 2 standard deviations.

require extensions of the SSPs in the database; we follow the prescription of [69] for each baseline, see Figure 2.

2.1.3 Damage functions

Our climate damage calculation can be broken down into three components: an *aggregate* climate damage, owing to the total damages incurred by climate change (i.e., labor disutility, mortality risk, or agricultural loss); a *tipping point* climate damage, which accounts for damages which are incurred by, for example, permafrost melt or Amazon dieback; and a *penalty function* which dissuades individual agents in our model from over-mitigating CO₂ concentrations in the atmosphere.

Aggregate climate change damages

Aggregate damages (as a function of % global GDP in 2020) are defined as global damages owing to climate change, and their magnitude is estimated in AR6 by WGII [43] (see their Figure Cross-Working Group Box ECONOMIC.1, panels (a)-(c), p. 16-114). We specify three aggregate damage functions in particular: one that is modeled after statistical climate damage modeling efforts [8] (panel (a) in Figure Cross-Working Group Box ECONOMIC.1), one estimated using structural estimation techniques [89, 95] (panel (b) in Figure Cross-Working Group Box ECONOMIC.1), and a meta analysis of climate damage estimates [41] (panel (c) in Figure Cross-Working Group Box ECONOMIC.1), such that for each we have

$$\mathcal{D}(T') = T'(\varpi_1 + \varpi_2 T') \quad (2.6)$$

where $\varpi_1, \varpi_2 \in \mathbb{R}^+$ are fitted coefficients. (Note there is no zeroth order term, as $D(T' = 0) = 0$ is required.) We refer to each of these damage functions by their estimation methodology in what follows, i.e., “the statistical damage function” and so on. We detail our methodology for fitting coefficient values

to the data in Appendix A, supply the fitted coefficients and their uncertainty in Table 1, and present the data and fitted curves in Figure 3. It should be noted that each of these damage functions come with limitations and qualifications, and in the case of the statistical damage function, we deviate from the IPCC representation in important ways. We discuss each damage function below.

Statistically estimated damage function. [8] The statistically estimated damage function builds on previous work involving the nonlinear response of economic productivity to temperature [9], following methodologies laid out more generally in [12]. This damage function relies on the specification of a certain horizon where damages set in, and choose the natural markers of 2049 and 2099 (mid-century and end of century, respectively). The mid-century and end of century estimates are starkly different, as in this framework climate change slows economic growth, therefore requiring sufficient time for damages to compound. Damages are also different depending on which SSP one chooses; this owes to the fact that each SSP contains different assumptions around adaptation, technological growth, and so on. Finally, the warming levels represented in [8] are relative to a 1986–2005 baseline, *not* relative preindustrial temperature levels. The IPCC’s representation of this damage function differs from the original publication in three ways: they only report end-of-century estimates; they aggregate damage estimates across SSPs without indicating the differences between each; and they report the temperature change as relative to preindustrial rather than to a 1986–2005 baseline.

We correct these inconsistencies in our formulation to be consistent with the original publication. We include explicitly the time dependence of this damage function in our simulated climate damages, allowing for the decision period of 2030 and 2060 to use the mid-century estimates and each decision period from 2100 onward to use end of century estimates. This of course is not perfect, as damages are expected to continue growing past 2100 in their framework, but we lack projection data to extend their framework to longer time horizons. Therefore, our estimates of climate damages in the long run are to be considered as conservative. We also change the fit to damage function data based on which SSP we consider. Finally, we correct the temperature baseline by shifting the abscissa by ~ 0.8 °C to correctly represent temperature anomalies relative to preindustrial.

A final qualifier to our use of this damage function is our parameterization of uncertainty. The uncertainty range for these estimates is large, and net-benefits of climate change are not ruled out even in the long term (though they are exceptionally rare). The extent of this uncertainty is largely driven by the assumed economic response to climate change and the discount rate chosen in their model, and no range is given for the estimates of economic damages for a given climate model’s projection; only the median estimate is reported for each climate model. We also suppress climate model uncertainty in their presented results so as to not double count climate uncertainty, resulting in a more narrow uncertainty envelope for damages estimates. In view of these qualifications, we take a simplified approach to assigning uncertainty in these estimates by (1) assigning uncertainty around median estimates only, and (2) assuming uncertainty broadens between 2049 and 2099. See Figure 3A for our presentation of the statistically estimated damage function (assuming SSP2).

Structurally estimated damage function. [89, 95] In the case of the structurally estimated damage function, three integrated assessment models’ (DICE [76], PAGE [39], and FUND [97]) output are aggregated to form a range of climate damages estimates as a function of temperature. However, it is unclear if this aggregation process is reliable, as the range of climate damage estimates from each model

can be traced back to different components of individual models, such as climate representations and discount rates [89]. We take the aggregation of damage estimates at face-value, and do not differentiate between the different models used to estimate the damages, see Figure 3B.

Meta-analytic damage function. [41] The meta-analytic damage function is simply a synthesis of studies found in the literature, and though care was taken to account for duplicates of studies and methodology, it is unclear if a set of damage estimates using different models and estimation types can be joined together in this way to form one unified “damage function.” It is also unclear if the resulting uncertainty can truly be labeled as “parametric” or simply a by-product of disagreements in the literature. Nonetheless, we assign a simple envelope of uncertainty to the preferred damage function of [41], see Figure 3C.

The limitations described above and the inability to properly compare damage estimates across studies and methodologies led WGII to conclude that a reliable range of damage estimates could not be determined; put differently, there is no “right” damage function that we can specify in this work [43]. We resolve this issue by taking a conservative approach and sampling all of the damage functions mentioned above with equal probabilities; in this way, we remain agnostic about which damage function is the “right” one, and sample the space of possible damage functions in addition to uncertainty inherent to a specific climate damage estimation methodology.

Despite the issues with individual damage functions described above, our approach to sampling all of the damage functions has the benefit that, at minimum, we sample a variety of damage function shapes and scales. The statistically estimated damage function has a convex shape, implying that climate damages set in quickly before leveling out in time. Furthermore, this damage function is time dependent, capturing the impact of climate change impacting economic growth; this has been shown to be an important factor in climate policy [71]. The structurally estimated damage function, in contrast, is concave, with low damages in the short run which slowly rise over time. Finally, the meta-analytic damage function is also concave, but rises much faster than the structurally estimated damage function. This variety in damage function shape and scale allows us to highlight the impact of damage function shape on price paths in § 3.

Tipping point damages

In addition to the aggregate damages accrued owing to climate change, an additional damage potential exists for climate-related tipping points, such as permafrost melt or Amazon dieback. Moreover, the probability that such a tipping point would occur and accelerate economic damage increases with global mean surface temperature. Thus, we include an additional piece of our damage function owing to these tipping points, $\mathcal{D}_{tp}(T')$, taken from [20] (see their Figure 5c), such that the total damages are given by

$$\mathcal{D}_{tot}(T') = \mathcal{D}(T') + \mathcal{D}_{tp}(T'). \quad (2.7)$$

Note that $\mathcal{D}_{tp}(T')$ has the same functional form as the aggregate damage function, i.e., Eqn. (2.6). See Figure 3D for a visualization and Table 1 for the coefficients of this damage function and corresponding uncertainties.

Table 1: Damage function coefficient parameter values and uncertainties. Fitted parameters for the damage function (2.6) based on [43] and [20].

Damage function	$\bar{\varpi}_2 [K^{-2}]$	$\sigma_{\varpi_2} [K^{-2}]$	$\bar{\varpi}_1 [K^{-1}]$	$\sigma_{\varpi_1} [K^{-1}]$
Statistically estimated [8]				
SSP1, mid-century	5.36×10^{-3}	7.13×10^{-4}	8.93×10^{-3}	1.12×10^{-3}
SSP2, mid-century	3.09×10^{-3}	4.76×10^{-4}	1.24×10^{-2}	1.90×10^{-3}
SSP3, mid-century	2.95×10^{-3}	4.74×10^{-4}	1.18×10^{-2}	1.89×10^{-3}
SSP4, mid-century	3.50×10^{-3}	7.14×10^{-4}	5.83×10^{-3}	1.19×10^{-3}
SSP5, mid-century	3.40×10^{-3}	5.20×10^{-4}	1.14×10^{-2}	1.75×10^{-3}
SSP1, end-of-century	-1.24×10^{-3}	2.49×10^{-4}	7.07×10^{-2}	1.42×10^{-2}
SSP2, end-of-century	-2.33×10^{-3}	4.75×10^{-4}	7.21×10^{-2}	1.47×10^{-2}
SSP3, end-of-century	-2.81×10^{-3}	5.93×10^{-4}	7.20×10^{-2}	1.52×10^{-2}
SSP4, end-of-century	-1.11×10^{-3}	3.42×10^{-4}	4.67×10^{-2}	1.43×10^{-2}
SSP5, end-of-century	-1.33×10^{-3}	3.45×10^{-4}	5.56×10^{-2}	1.45×10^{-2}
Structurally estimated [89, 95]	2.30×10^{-3}	8.53×10^{-4}	2.05×10^{-3}	7.59×10^{-4}
Meta analysis of climate damages [41]	6.85×10^{-3}	2.43×10^{-3}	2.98×10^{-4}	1.06×10^{-4}
Climate tipping points [20]	4.8×10^{-1}	4×10^{-2}	-4×10^{-2}	1×10^{-2}

Penalty function

The last component of our damage calibration includes a penalty function, $\mathcal{D}_{pen}(\mathcal{C}_t)$, which, unlike our aggregate and tipping point damage functions, relies on the CO₂ concentrations rather than GMST. The reason is that the penalty function is intended to disincentivize individual agents from over mitigating the amount of CO₂ in the atmosphere, thus driving CO₂ concentrations below that of preindustrial. (The issue of global cooling is, after all, secondary to global warming, at least for now.) In this spirit we write the penalty function as

$$\mathcal{D}_{pen}(\mathcal{C}_t) = \left(1 + e^{k(\mathcal{C}_t - m)}\right)^{-1}, \quad (2.8)$$

where $m = 200$ ppm accounts for half the penalty accrued and $k = 0.05$ is set to ensure smoothness. This combination of free parameters guarantees that $\mathcal{D}_{pen}(\mathcal{C}_t = 280 \text{ ppm}) \approx 0$ while, for example, $\mathcal{D}_{pen}(\mathcal{C}_t = 150 \text{ ppm}) \approx 0.924$.

Sampling damage function uncertainty

We sample uncertainty in the damage function in two ways. The first is by sampling the parametric uncertainty in each damage function; that is, the uncertainty in the values of ϖ_1, ϖ_2 in (2.6) (see Appendix A for details). The distributions of ϖ_1, ϖ_2 are assumed Gaussian with mean and variance provided in Table 1, and we take three million Monte Carlo samples.

The second source of uncertainty in the damage function pertains to which damage function (i.e., statistical, structural, or meta-analytic) we specify in the first place. IPCC WGII makes no recommendations in this regard. We therefore assign a hyper-parameter in our simulated climate damages that randomly chooses a damage function. Given that we take three million draws in our Monte Carlo sampling of parametric uncertainty, allowing for three damage functions still on average corresponds to a million samples of each damage function's parametric uncertainty, a more than representative sample. This methodology allows us to remain agnostic with respect to which damage function we choose, and examine the consequences of our agnosticism on carbon price paths in § 3.

Calculating damages at a particular decision node

Climate damages depend on the global mean surface temperature anomaly. However, a representative agent in our model at a given decision node only knows the possible *end* states which can be accessed from her state. She does not know the exact fragility at her own node, or any θ_t for $t \leq T$, owing to the inherent uncertainty surrounding both the climate system (such as the precise value of TCRE) and economic impacts (such as damage functions). In this way, the tree emanating from her current node can be thought of as a *sub-probability landscape* of the entire tree, where θ_t characterizes the risk inherent to the entire sub-landscape. If this landscape contains within it an equal number of high and low fragility end states, the fragility is considered to be average; if it only contains end states with high fragility, for example, then the fragility is high. The same logic follows with low fragility states. Owing to the agent not knowing the current fragility, the damages assessed at her decision time are dependent on *proxies* for the relevant damage variables. The two proxies used in our model is the fragility θ_t

(which tells us which end states are accessible) and the cumulative CO₂ emissions, Ψ_t (which tells us *approximately* how warm the world *should* be, but does not immediately map to the temperature at time t owing to uncertainty in the TCRE). These two variables in concert gives us a basis from which we can interpolate end state climate damages backwards in time to any decision node. In addition, the mitigated emissions pathway enables us to calculate the CO₂ concentrations at the individual's decision time, enabling evaluation of (2.8).

We therefore calculate the damage at a given node as a probability-weighted average of the current-period damages accessible to each end node across states of fragility, plus the penalty function, such that

$$\mathcal{D}_{node}(\Psi_t, \theta_t, \mathcal{C}_t) = \sum_{\theta_T} P(\theta_T | \theta_t) \mathcal{D}_{tot}(T', \theta_t) + \mathcal{D}_{pen}(\mathcal{C}_t). \quad (2.9)$$

2.1.4 Cost of mitigation

Calculating the cost of mitigation requires specifying a marginal abatement cost curve (MACC), which relates the price of abatement to the fraction of emissions abated. However, such a curve will vary depending on three factors [29]: (1) the current state of emissions mitigation technologies, which in aggregate represent the abatement potential (in GtCO₂-eq yr⁻¹) as a function of cost, (2) the availability of a backstop technology, which allows for net-negative emissions, and (3) technological advancement, which makes mitigation costs cheaper over time. We take each component – formulating a baseline MACC based on current abatement technologies, accounting for backstop technology, and incorporating technological advancement – in turn below.

Marginal abatement cost curve estimation

Estimating a MACC requires a functional relationship between the fraction of emissions abated, x , the per-ton tax rate, τ , and the emission pathway, E . We use the most recent estimates for the cost of CO₂ emission abatement presented in AR6 WGIII [44] (see their Figure SPM.7, p. SPM-50). Note that the data presented by WGIII are for mitigation costs in terms of the 2030 abatement potential. We make three important assumptions in interpreting the data from AR6 WGIII. The first is that we assume cost estimates are additive, which is not necessarily the case; however, we expect changes in costs and abatement potential to be small enough to consider them as negligible in this study. The second is that we neglect negative costs; that is, whenever WGIII data dictates that costs are < \$0, we set the cost to zero. The final assumption is that for abatement potentials outside the range provided by the IPCC, we assume the functional relationship between τ and x established for lower abatement potentials holds. With these assumptions in mind, we fit an exponential curve to the cost data (see Figure 4A), such that

$$\tau(x) = \tau_0 \left(e^{\xi x} - 1 \right), \quad (2.10)$$

where $\tau_0, \xi > 0$ are constants.

In the final analysis, we are interested in the total cost to society, $\kappa(\tau)$ for each particular tax rate τ , in units of the fraction of 2020 consumption lost. We closely follow the formulation in [19] and use the envelope theorem to calculate $\kappa(\tau)$. We assume a representative agent optimizes consumption $c(\tau)$

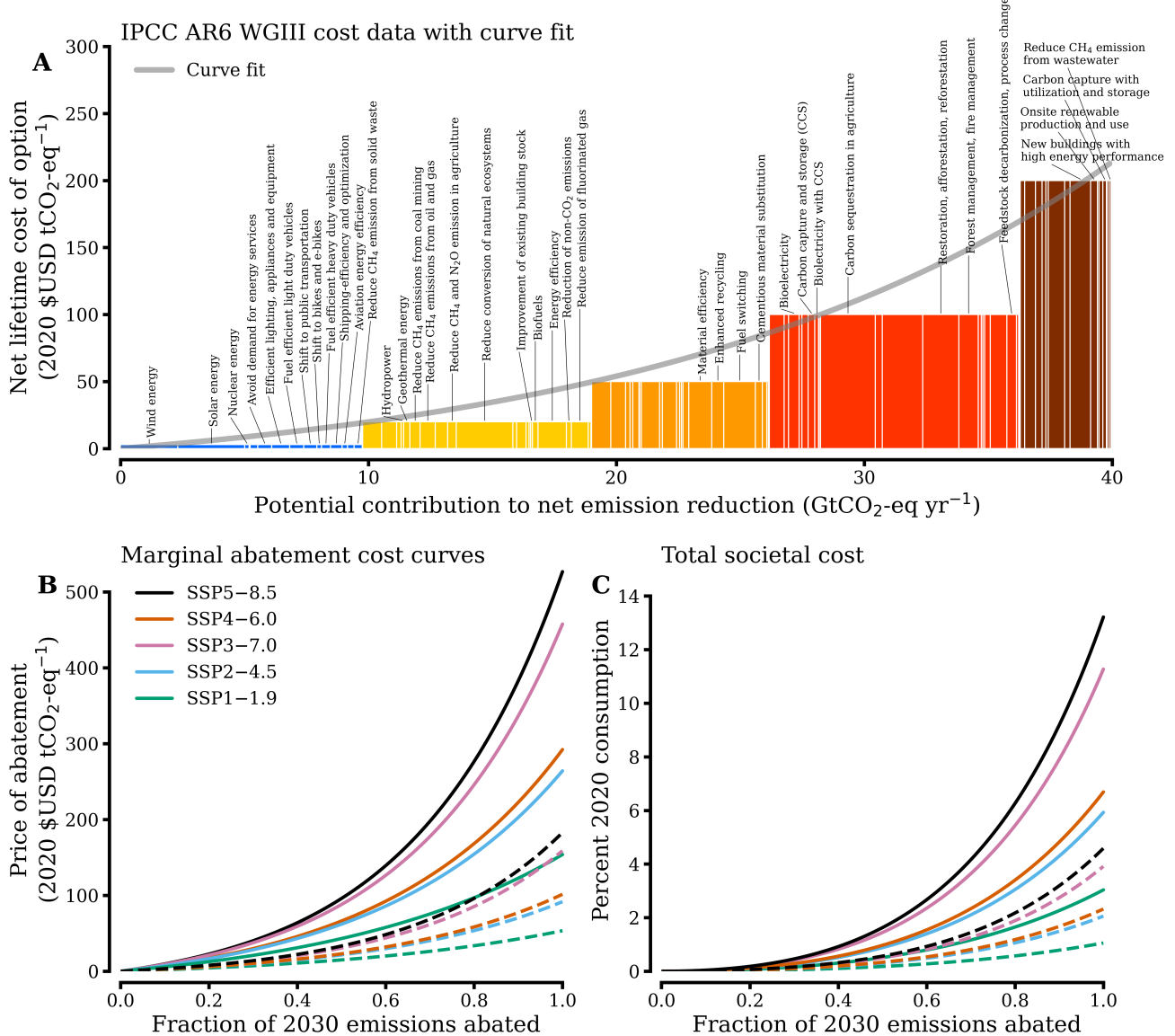


Figure 4: Cost of mitigation. Panel A shows the mitigation potential and cost for each methodology given by the IPCC using their WGIII data. Blue represents zero costs (listed as negative in AR6), yellow is \$0 - \$20 range, orange is \$20-\$50, red is \$50-\$100, and maroon is \$100-\$200. Note that the methodology label is only on the bar with the most mitigation potential for said methodology. Our curve fit is in grey. Panel B shows the fitted marginal abatement cost curves given by (2.10) and Panel C shows the total cost to society given by (2.14) using our ‘main specification’. Panels B–C use values from Table 2. In panels B–C, solid lines correspond to 2030, while dashed lines are cost curves in 2100, assuming an exogenous technological growth rate of 1.5% and no endogenous technological growth.

such that $dc(\tau)/d\tau = -E(x(\tau)) = -E(\tau)$, where we have dropped the dependence of the emissions on mitigation action for clarity. Then by simple integration the consumption is given by

$$c(\tau) = \bar{c} - \underbrace{\int_0^\tau E(\zeta)d\zeta}_{=:K(\tau)}, \quad (2.11)$$

where $\bar{c} > 0$ is the baseline endowed consumption and $K(\tau)$ is the cost to society in monetary units (i.e., dollars). Eqn. (2.11) would be correct if the government was to waste the entirety of the policy proceeds, given by $E(\tau)\tau$. We instead assume that the proceeds are refunded in a lump sum [63], thus requiring an alteration to $K(\tau)$ such that

$$K(\tau) = \int_0^\tau E(\zeta)d\zeta - E(\tau)\tau. \quad (2.12)$$

The lump sum refund does not allow for CO₂ tax proceeds to be used to decrease distortionary taxes unrelated to CO₂ emissions; this would lower the *net* cost of CO₂ even further [31, 52]. Rewriting the emissions as $E(\tau) = E_0(1 - x(\tau))$ where E_0 is the (SSP-dependent) 2030 emissions in GtCO₂ yr⁻¹, we have

$$K(\tau) = E_0 \left(\tau x(\tau) - \int_0^\tau x(\zeta)d\zeta \right). \quad (2.13)$$

Note that E_0 is the 2030 emissions for consistency with the cost data presented by WGIII. Now using (2.10) and its inverse in (2.13), carrying out the integral, and dividing by 2020 consumption results in the total cost to society in terms of fractional 2020 consumption loss, given by $\kappa_{MACC}(x)$, as

$$\kappa_{MACC}(x) = \frac{E_0\tau_0}{c_{2020}} \left(\frac{e^{\xi x} - 1}{\xi} - x \right), \quad (2.14)$$

where c_{2020} is the 2020 global consumption in billions of 2020 \$USD, set to 61880 (taken from the [World Bank](#)). A table of fitted values for τ_0 and ξ for each SSP are provided in Table 2, as well as a calculation for the percent of consumption required to abate all emissions. Fits for (2.10) are shown in Figure 4B.

Backstop technology

Our model represents backstop technology via permitting CO₂ removal [54, 73]. CO₂ removal occurs whenever the mitigation exceeds unity; this leads to negative emissions and thus carbon removal from the atmosphere. The price of carbon removal has a major source of uncertainty in assessing future climate policy [50, 92, 57, 58, 40], with estimates ranging from \$50 – \$1000 2020 USD per ton of CO₂ removed. Recent estimates are more promising, however, with per ton price of CO₂ removal ranging between \$94 – \$232 [54]. Regardless of the specific dollar estimates provided in the literature, backstop technology faces a common hurdle: scalability [37]. The parameter x in our MACC is the fraction of *2030 emissions abated*; therefore, removing even a small percentage of these emissions from the atmosphere is equivalent to abating billions of tons of CO₂ from the atmosphere in short order. The technology to carry out this task is simply unavailable at present. We take a simple approach to

Table 2: Marginal abatement cost curve parameters. Fitted coefficients for (2.10), the cost of abating all emissions, $\tau_a := \tau(x = 1)$, and the percent of consumption required to abate all emissions, $\kappa_a := \kappa_{MACC}(x = 1)$, based on AR6 WGIII data for each SSP in our ‘main specification’ and our “no free lunches” alternative calibration.

SSP	ξ	τ_0 [2020 \$USD tCO ₂ -eq ⁻¹]	τ_a [2020 \$USD tCO ₂ -eq ⁻¹]	κ_a [%]
Main specification				
1	1.9	27.5	153.88	3.0
2	2.4	27.5	264.09	5.9
3	2.9	27.5	457.57	11.3
4	2.5	27.5	292.15	6.69
5	3.0	27.5	526.58	13.2
“No free lunches”				
1	1.8	58.9	297.42	6.1
2	2.3	58.9	528.58	11.9
3	2.8	58.9	909.69	22.5
4	2.3	58.9	528.58	13.4
5	2.9	58.9	1011.56	26.3

adjusting our cost curve to account for backstop technology by imposing a *backstop technology premium*, $\tau_{BS} > 0$, which is an extra price for carbon removal which shifts τ_0 to $\tau_0 \rightarrow \tau_0 + \tau_{BS}$. In the base case, we essentially price out to-scale backstop technology before 2100, setting τ_{BS} to be \$10000 2020 USD. This alters our MACC cost curve (2.14) when $x > 1$, such that

$$\kappa_{MACC}(x) = \begin{cases} \frac{E_0 \tau_0}{c_{2020}} \left(\frac{e^{\xi x} - 1}{\xi} - x \right), & 0 \leq x \leq 1, \\ \frac{E_0 (\tau_0 + \tau_{BS})}{c_{2020}} \left(\frac{e^{\xi x} - 1}{\xi} - x \right), & x > 1. \end{cases} \quad (2.15)$$

Technological progress

Technological progress in our model is captured by allowing the cost of mitigation to society $\kappa_{MACC}(x)$ to decrease in time as technological proficiency makes mitigation cheaper. Technological progress can occur in two ways: (1) exogenously, where general technological improvement independent of agent choices make mitigation cheaper, and (2) endogenously, where if a given individual invests in mitigation early, the cost of mitigation goes down more over time [1]. The exogenous (endogenous, resp.) technology advancement rate is given by $\varphi_0 \geq 0$ ($\varphi_1 \geq 0$, resp.). Incorporating these factors

into our cost curve results in our final expression for the cost of mitigation to society,

$$\kappa_t(x) = \kappa_{MACC}(x) (1 - \varphi_0 - \varphi_1 X_t)^{t-10}, \quad (2.16)$$

where

$$X_t := \frac{\int_0^t x(\zeta) E(\zeta) d\zeta}{\Psi(t)}, \quad (2.17)$$

is the weighted average mitigation up to time t . Note the technological growth factor is offset by ten years as the cost data from AR6 is for 2030 technologies. The inclusion of (2.17) captures how an individual's decisions up to a given time impact the cost curve; if an agent increases her average mitigation, thus abating more emissions, costs decrease quicker than if she hadn't abated at all.

“No free lunches”

Estimating the cost of CO₂ abatement is a notoriously challenging task. The cost estimates presented above are static, in the sense that they represent the costs of the lifetime of the project and, for example, ignore spillover effects [44]. However, static estimates fail to capture the impact of the costs (or savings) associated with a given project that outlive the project lifetime itself [29]. We partially resolve this issue by including technological growth and learning, but this only serves to bring static costs down. It is entirely possible that the static cost of a given option could be low, while its dynamic cost could be relatively high; building large-scale, inefficient yet presently cheap technologies that are locked-in in the long term provides an illustrative example of this effect.

Such considerations lead some to argue that costs should not be estimated from the “bottom up” as done here, but rather from the “top down.” This, for example, is the case in DICE–2016R and similar climate-economic models [77, 78]. Such estimates generally paint a more pessimistic picture than the “bottom up” methods, positing that the cost of abating CO₂ emissions is actually quite larger than adding up the cost of each individual option, owing to inertia and friction in the economic system, a set of barriers typically summarized as the “energy paradox” [48, 3].

For example, “bottom up” estimates generally find methodologies with significant abatement potential and close to zero or negative cost; AR6 finds ~ 10 GtCO₂-eq worth of abatement for $\leq \$0$. That’s almost 25% of all CO₂-eq emissions in 2021 [45]. The question is, then, why weren’t each of these methods implemented yesterday? The answer must be an amalgam of inertia, friction, and sub-optimal policy and incentive structures ‘in the real world.’

To address this concern, we perform a sensitivity test to the output of CAP6 by recalibrating the MACC to exclude zero-cost abatement technologies. This calibration does not serve as our ‘main specification,’ however, as the recalibration procedure is *ad hoc* and not grounded in any particular estimation methodology. Therefore, we use the IPCC-data calibrated MACC (the ‘main specification’ parameters in Table 2) for the purpose of assessing ‘optimal’ policy in CAP6.

We perform our recalibration by shifting all of the mitigation potential in the IPCC dataset up by one cost bracket; for example, the zero cost methodologies (the blue bars in Figure 4) now have \$20 2020 USD tCO₂-eq⁻¹ life time cost, and so on. The highest cost abatement technologies are set to cost 400 2020 \$USD tCO₂-eq⁻¹. We coin this MACC calibration as the “no free lunches” MACC, and provide

its parameter values in Table 2. The analogous figure to Figure 4 for the “no free lunches” MACC is provided in the *Supplementary Information*.

Note we perform a second recalibration that sets the costs of the the < \$0 mitigation options to infinity, coined the “infinite cost” calibration. The figure associated with this calibration is in the *Supplementary Information*. We do not show the results of CAP6 with this calibration as the final costs of abatement are lower than in the “no free lunches” case in Table 2. Hence, the results will simply be an interpolation between the main specification and the “no free lunches” results.

2.2 Climate model

Here we present the climate component of our model in two parts. The first subsection details our implementation of the transient climate response to emissions that maps emissions to temperature anomalies above preindustrial, see (2.19). The second subsection outlines our impulse response function approach to modeling the carbon cycle, given by (2.23). The numerical values of relevant climate parameters are found in Table 3. Throughout, we refer to $E(t)$ as a general emissions pathway; in practice, this is a (potentially mitigated) SSP emissions baseline.

2.2.1 Mapping emissions to temperature anomaly above preindustrial

We map CO₂ emissions to the temperature anomaly above preindustrial levels, denoted as T' , using the *transient climate response to emissions* (TCRE) [4, 64, 68, 28, 62]. The TCRE is defined as a linear scale factor $\lambda > 0$ that maps the cumulative CO₂ emissions, $\Psi(t) := \int_0^t E(\zeta)d\zeta$, to temperature. The physical basis for TCRE is a compensation between the diminishing sensitivity of radiative forcing to CO₂ at higher atmospheric concentration and the diminishing ability of the ocean to take up heat and carbon at higher cumulative emissions [42].

Generally, one defines the TCRE as the ratio to present-day warming to cumulative emissions above preindustrial to date; however, this ratio alone underestimates warming owing to other greenhouse gases having been emitted since preindustrial. An additional correction is therefore required to λ owing to non-CO₂ forcing from other trace gases, such as methane and nitrous oxide [17, 42]. We follow the framework laid out in [17] and include a non-CO₂ forcing term $f_{nc} > 0$ that increases the average value and variance of the TCRE estimate provided by the IPCC. We write our “effective” TCRE – the TCRE including non-CO₂ forcing factors – as

$$\lambda_{eff} := \frac{\lambda}{1 - f_{nc}}. \quad (2.18)$$

The mean value of λ , f_{nc} , and λ_{eff} and their uncertainties are provided in Table 3. Using this approach, we are able to reproduce central estimates of warming levels this century reported by WGI in AR6 for each SSP reasonably well (see the *Supplementary Information* and their Table 4.5, p. 582 [42]). A limitation of our approach, however, is an excess of uncertainty in our end-of-century projections, as the combination of uncertainty in non-CO₂ forcing and TCRE itself convolve to widen the range of possible temperature rise by the end of the century that is not seen in more complete, complex

climate models. This hardly impacts middle-of-the-road emissions scenarios such as SSP2–4.5, but is prevalent in high emissions scenarios such as SSP5–8.5. As λ_{eff} is assumed Gaussian, this widening of uncertainty does not significantly impact risk assessment (as there is equal chances of a “good” or “bad” draw of λ_{eff}), but it is nonetheless an important qualification to our approach. Therefore in our calculations of temperature, we use

$$T'(t) = \lambda_{eff} \Psi(t). \quad (2.19)$$

2.2.2 Carbon cycle model

For a given emission time series the corresponding CO₂ concentration time series can be found by convolving emissions with the impulse response function (IRF) of a pulse of CO₂ emissions, denoted as $\mathcal{I}(t)$, such that

$$\mathcal{C}_E(t) = E(t) * \mathcal{I}(t). \quad (2.20)$$

The IRF provides the time dependent fractional concentration of CO₂ after a pulse is emitted into the atmosphere. Convolving the emission time series with the IRF hence allows us to accurately track the decay of the emission at each time step [96]. In [51], it is shown that the IRF for a pulse of CO₂ can be sufficiently represented by a superposition of exponentials, given by

$$\mathcal{I}(t) := a_0 + a_1 e^{-t/\tau_1} + a_2 e^{-t/\tau_2} + a_3 e^{-t/\tau_3}. \quad (2.21)$$

See Table 3 for the numerical values of the fitting coefficients a_i and timescales τ_i in (2.21). Hence, we use (2.21) in (2.20) to find the concentrations of CO₂ after 2020.

The final component of the concentration time series accounts for pre-2020 CO₂ that is present in the atmosphere when an agent begins emitting. This ensures that our carbon cycle model not only acts to take new CO₂ out of the atmosphere, but continues to remove CO₂ from past emissions. To account for this extra CO₂ in the atmosphere, we make the assumption that the majority of CO₂ before 2020 is old, such that the time it has been in the atmosphere is much greater than τ_2 . This implies that there is a constant fraction that remains, and a piece that is still decaying; the CO₂ that decayed through the τ_2 and τ_3 channels has been set to zero. Hence, the remaining CO₂ in the atmosphere is given by

$$\mathcal{C}_{pre-2020}(t) = \mathcal{C}_{2020} \left(\frac{a_0 + a_1 e^{-t/\tau_1}}{a_0 + a_1} \right), \quad (2.22)$$

where $\mathcal{C}_{2020} = 420.87$ ppm.

Therefore, we can write the total carbon concentrations time series for a given individual as $\mathcal{C}(t) = \mathcal{C}_{pre-2020}(t) + \mathcal{C}_E(t)$, or

$$\mathcal{C}(t) = \mathcal{C}_{2020} \left(\frac{a_0 + a_1 e^{-t/\tau_1}}{a_0 + a_1} \right) + E(t) * \mathcal{I}(t), \quad (2.23)$$

which completes our model for carbon concentrations.

Table 3: Climate model parameter values and uncertainties. Values of fitting coefficients a_i and timescales τ_i used in (2.21) (taken from [51]), as well as the best estimate and standard deviation of TCRE (taken from [42]).

Fitting Coefficient		Timescale [years]	
a_0	0.2173	τ_1	394.4
a_1	0.2240	τ_2	36.54
a_2	0.2824	τ_3	4.304
a_3	0.2763		
TCRE Parameters			
$\bar{\lambda} = 0.45 \text{ } ^\circ\text{C (1000 GtCO}_2)^{-1}$		$\sigma_\lambda = 0.18 \text{ } ^\circ\text{C (1000 GtCO}_2)^{-1}$	
$\bar{f}_{nc} = 0.14$		$\sigma_{f_{nc}} = 0.11$	
$\bar{\lambda}_{eff} = 0.52 \text{ } ^\circ\text{C (1000 GtCO}_2)^{-1}$		$\sigma_{\lambda_{eff}} = 0.21 \text{ } ^\circ\text{C (1000 GtCO}_2)^{-1}$	

2.3 Prototypical model run

Given that our climate-economy model is unlike most other such models in the literature, an example of how each of the components laid out above interact in one model “run” is warranted. First, let us establish some important concepts and recurring values that will be essential for our understanding. First, we have chosen $T = 6$ decision periods. This implies that we have a total of $n := 2^T - 1 = 63$ decision nodes in the tree. Decisions are made at times t such that $t \in \{2020, 2030, 2060, 2100, 2150, 2200\}$, and an additional period (with no decisions being made) occurs at $t = 2250$ to establish the terminal period conditions. As the binomial tree is path dependent, it immediately follows that the number of unique paths through the tree is equal to the number of nodes in the *final* period, given by $n_f := 2^{T-1} = 32$. Any vector of length n (which represents the value of a given variable, say mitigation, at each *node* in the tree) can be readily translated into a set of *paths* of shape $n_f \times T$ through the tree (which represents the values of a given variable at the nodes in each *path* through the tree). Note that Figure 1 is a helpful visual guide for our entire discussion.

Step 1: Simulate climate damages

The first step is to simulate potential climate damages. This comes *before* agent utility is optimized, as decisions about utility are made *within the context* of the landscape of potential damages. Once the landscape of damages are calculated (and we will be more precise about what is meant by “landscape” in our discussion below), then damages are interpolated in our utility calculations. Note that in the following discussion $N_{MC} = 3 \times 10^6$ refers to the number of draws taken in our Monte Carlo samples of TCRE and damage function parametric uncertainty.

Climate damages are simulated using the following prescription. First, we specify an emissions baseline by choosing an SSP. Once specified, there is a range of possible cumulatively emitted CO₂ at each point in time, depending on hypothetical agent mitigation policy. Let the maximum cumulative emissions (associated with no mitigation) at a time t be represented by Ψ_t^* . Cumulative emissions Ψ_t therefore

always lie in the range $0 \leq \Psi_t \leq \Psi_t^*$. We discretize the range of potential cumulative emissions at each point in time by applying a constant scaling $0 \leq m \leq 1$ to the SSP and computing damages for each value of m . In our runs, we choose $M = 101$ values of m . To recapitulate: we choose a value of m such that $0 \leq m \leq 1$, resulting in a time series of cumulative emissions $\Psi_t = m\Psi_t^*$ that is manifestly less than or equal to the maximum permissible amount Ψ_t^* for all t .

For a given time series of cumulative emissions, the corresponding temperature change is uncertain owing to the uncertainty in the TCRE. We draw N_{MC} samples of the TCRE from a rectified normal distribution with best estimate and variance taken from Table 3 and evaluate (2.19), which results in N_{MC} time series of global temperature change. For each temperature time series, we at random choose a damage function (statistical, structural, or meta-analytic) and evaluate (2.6) for the chosen damage function and the additional tipping points piece. The total damage is given by (2.7). This procedure results in N_{MC} time series of climate damages. The climate damage time series are then ordered by severity of the final period damages (thus establishing an orientation of the “fragility” dimension), and grouped in N_{MC}/n_f sized bundles. An average is then taken over each bundle, resulting in n_f time series of climate damages. The averaging procedure is necessary to make the simulated climate damages congruent with the dimensionality of the binomial tree.

The procedure described above has resulted in a $n_f \times T$ matrix of climate damages, ordered from high to low. Continuing for every value of m results in a $M \times n_f \times T$ *landscape* of climate damages. This is coined as a landscape owing to its encapsulation of the potential extent of climate damages. The M -dimension contains information about the extent of emissions; the T -dimension contains information about the timing of damages; and the n_f -dimension contains the extent of climate damages based on the uncertainty in TCRE and the damage function. With this landscape now calculated, we can turn our attention to how the economic utility is maximized within it.

Step 2: Utility maximization

We optimize the economic utility given by (2.1) using a genetic algorithm [30, 70, 53]. The genetic algorithm is a stochastic optimization routine, where a set of random solution vectors are generated and their “fitness” is determined. The vectors with high fitness are stored for the next round (they “survive”), and vectors with low fitness are discarded (they “die”). The low fitness vectors are replaced with another set of random vectors (the “offspring” of the more fit vectors) whose fitness is compared to the incumbents’. This process continues until minimal changes in the highest fitness value are recorded for a number of rounds; the vector corresponding to the highest fitness is then said to be the “optimal” solution vector. The genetic algorithm is best suited for objective functions with unknown or difficult to evaluate gradients, making it ideal for CAP6. In our use case, the randomly selected solution vectors are mitigation vectors, and a given vector’s fitness is its 2020 economic utility. In what follows, allow \vec{x} be a vector of mitigation values with length n .

EZ utility captures future risk by allowing the utility at time t be dependent on the utility at time $t+1$ (see Eqn. (2.1)). Evaluating the utility must therefore begin at the final period, and is then evaluated *backwards* to $t = 2020$. Thus, the first step is to evaluate the final period utility (2.2) where the final period consumption is given by (2.5) for each final state node. (Recall there are $n_f = 32$ nodes in the

Table 4: Term structures of preferred and featured runs. Here we show the term structures for each discount rate we employ in our featured and preferred CAP6 runs.

Ramsey discount rate [%]	δ [%]	η
2 (<i>Preferred</i>)	0.2	1.20
1.5	0.1	0.93
2.5	0.5	1.42
3	0.8	1.53

final period.) The assumed SSP and the mitigation vector \vec{x} are used to calculate the emissions time series for every path through the tree, and thus the CO₂ concentrations for each path using (2.23) and cumulative emissions at each end node. The cumulative emissions and carbon concentrations are used in (2.9) to calculate the damages at each node.

For each node before the final period, the mitigation action *up to but not including* a given node is used to calculate the level of CO₂ concentrations using (2.23) and the cumulative emissions at that node. The cost of mitigation is found using (2.16), and the damages are found using (2.9). These in tandem determine the consumption by (2.4). The consumption and the following period utility are used in (2.1) to determine the utility. This continues for each node, and each randomly generated vector, until the genetic algorithm finds the mitigation vector with the highest utility.

Step 3: Visualize model output

The most fit mitigation vector \vec{x}^* translates into the output shown in Figures 5, 6, 7, 8, and 9 in the following way. To calculate the cost, we apply (2.10) at each node, including the technological growth prefactor found in (2.16). We calculate the expected mitigation using (2.17). We use \vec{x}^* to calculate the emissions at each node, which readily translates into the concentrations at each node using (2.23) and the *expected* warming at each node using (2.19) assuming the mean value of TCRE. Economic damages for each node are calculated using \vec{x}^* in (2.9). Averaging over the cost, expected mitigation, emissions, temperature, CO₂ concentrations, and damage amount in each period gives the time series shown in Figures 5, 6, 7, 8, and 9.

2.4 Model calibration

In this subsection we discuss two calibrations of CAP6. The first regards what we refer to as our *featured* and *preferred* model runs. These results take values for the Ramsey-esque discount rate from the most recent climate economics calibration studies [75] and agent risk aversion calibrated to financial market data [91]. They also feature a modest emissions scenario (SSP2–4.5), and relatively conservative assumptions around technological growth. The second set of calibrations is for our *ensemble runs*, where we randomly sample the economic parameter space. We take each in turn below.

2.4.1 Preferred and featured runs

To calibrate CAP6, we use the Ramsey equation for the discount rate [82], $r_t = \delta + \eta g_t$, where g_t is the growth rate of consumption, $\eta = 1/\sigma$ is the coefficient of risk aversion, and δ is the pure rate of time preference (PRTDP). Previous analyses use a discount rate of 3% [14], but recent studies use 2% in light of recent economic trends (such as falling interest rates) and expert elicitation [15, 22, 75]. Indeed, New York State adopted a 2% discount rate in their social cost of carbon calculations [74]. There are a number of combinations of δ and η which result in a given discount rate, and how one chooses them determines the term structure of the model. We show our term structures for our preferred and featured model runs in Table 4; note that we assume a constant growth rate of consumption $g = 1.5\%$ for all runs. Allowing for time-dependent or uncertain growth is an interesting topic of future work.

The use of EZ preferences allows RA to be decoupled from EIS (and thus, η), resolving a paradox that arises when using vRM or constant relative risk aversion (CRRA) preferences more generally [2]. The paradox can be outlined as follows. Consider a highly risk averse individual. In the framework of CRRA preferences, this means η is large. However, by the Ramsey formula this immediately implies a large discount rate, implying that this very risk averse individual actually cares very little about future damages. EZ preferences decouple risk aversion along different dimensions, thus resolving the paradox. We here calibrate the PRTDP and agent EIS in the Ramsey discounting framework, in line with recommendations from the United States government [14], and utilize EZ preferences in order to address this paradox.

We calibrate our preferred and featured model runs as follows. We use a 2% Ramsey discount rate for our preferred run, in line with other state-of-the-art IAMs [83], following the term structure described in [99]. For our three featured runs, we again follow the term structures of [83, 99]; see Table 4 for specifics. For each discount rate, we assume that $\psi = 10$, in line with trends observed in the United States financial market [91]. For our emissions baseline, we choose SSP2–4.5, as it most closely aligns with recent emissions trends [34]. Lastly, we assume an exogenous technological growth rate of 1.5% [84] and no endogenous technological growth, owing to an inability to reliably calibrate the endogenous technological growth rate parameter φ_1 .

The choice of no endogenous technological growth makes our technological growth assumptions exceptionally modest, given the known link between agent investment in mitigation and rates of growth in clean sectors [47, 1, 7]. We probe the influence of including endogenous learning in the “learning by doing” sensitivity test below, where we set $\varphi_1 = 1.5\%$. This allows us to demonstrate how consumption spent on mitigation can influence mitigation prices, an important feedback mechanism [29].

2.4.2 Ensemble runs

While risk associated with temperature rise and damage function uncertainty are holistically evaluated in a given run of CAP6, other risk factors exist and are excluded, such as uncertainty in the rate of technological growth, or which exogenous emissions baseline or discount rate is assumed. Each of these represent a source of epistemic uncertainty and thus risk; indeed, not knowing how much CO₂ will be emitted over the next century, for example, strongly influences the range of possible climate realizations, and thus, climate-related risk [35, 59].

Table 5: CAP6 ensemble parameter ranges. Here we give the ranges of values for each of our model parameters sampled in our ensemble runs.

Parameter	Symbol	Range
Risk aversion	ψ	3 – 15
Elasticity of intertemporal substitution	σ	0.55 – 1.08
Pure rate of time preference	δ	0.1% – 1.47%
Exogenous rate of technological growth	φ_0	0% – 3%
Endogenous rate of technological growth	φ_1	0% – 3%

To probe the impact of assumptions associated with the discount rate, emissions baseline, and technological growth rate, we carry out a Monte Carlo analysis. We sample discount rates between the range of 1.5% and 4.25%; we chose the lower bound based on recent work [75], and the upper bound is the preferred rate used in DICE–2016R [78]. We translate this range of discount rates to EIS and PRTP ranges by bilinearly interpolating the term structures laid out in [99]. The value of agent RA is highly dependent on the conditions of its measurement, but RA has been measured to as high as 15 in wealthy countries and as low as 3 in European welfare states [91], which defines our range.

The exogenous and endogenous rates of technological change are nigh impossible to calibrate empirically. We therefore choose the modest upper bounds of 3% for both rates. For reference, DICE–2016R [78] chooses a rate of 1.5% for exogenous technological growth, but does not model endogenous technological change, despite it being shown to have a significant impact on carbon price dynamics [1]. Note that we use our ‘main specification’ MACC for the ensemble run analysis. We take a thousand samples of these parameters from a Latin Hypercube [65], resulting in a thousand time series of model outputs.

3 Results

3.1 Main specification

We show the preferred and featured model runs of CAP6 in Figure 5. We find that the preferred discount rate of 2% implies a high cost of carbon and very stringent abatement policies, see panel 5B. The cost of carbon declines over time; this, however, should not be confused with reduced abatement action over time. Rather, the declining dynamics of carbon prices can be entirely attributed to the improved ability to abate CO₂ emissions owing to technological growth (see Eqn. (2.16)). This set of mitigation actions leads emissions peaking in 2070, with CO₂ concentrations stabilizing before starting to decrease by mid-century. The expected global temperature change resulting from this emissions policy is less than 1.5 °C by 2100 (~ 1.47 °C) and less than 2 °C in 2200 (~ 1.6 °C). Finally, we find that agents on average lose about 2.2% of the world’s GDP by 2100, and lose about 2.7% total by 2200. To our knowledge, CAP6 is the first IAM that, in the absence of any normative calibrations, provides economic support for the warming targets established in the Paris agreement.

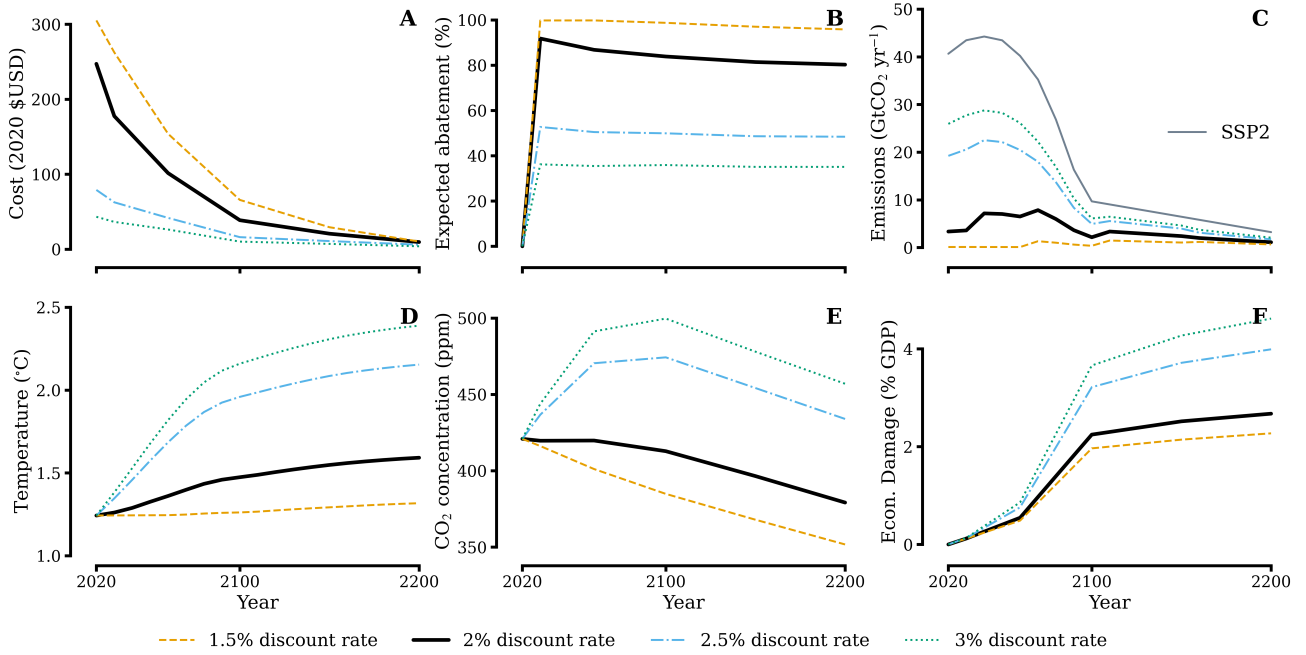


Figure 5: Preferred and featured model runs. We show model output for four discount rates: 1.5%, 2% (preferred), 2.5%, and 3%. Panel **A** shows the carbon price path, panel **B** shows the expected abatement level in percent, panel **C** shows the expected global CO₂ emissions, panel **D** shows the global mean surface temperature above preindustrial, panel **E** shows carbon concentrations, and panel **F** shows the incurred economic damages.

The impact of varying the discount rate is highlighted by our featured model runs. Decreasing the discount rate to 1.5% leads to complete and immediate cessation of emissions (see panel 5B), thus maximizing costs and decreasing 2100 (2200, resp.) warming by 0.2 °C (0.3 °C, resp.) in comparison to the 2% run. Larger discount rates relax the stringent abatement policies seen in the 2% and 1.5% discount rate cases. This results in lower costs and less mitigation action, and consequentially, larger warming and damages. Indeed, we find that both the 2.5% and 3% discount rates warm beyond the warming target of 1.5 °C by 2100 established in Paris. Moreover, the 3% discount rate policy exceeds 2 °C warming by 2100, and the 2.5% discount rate policy barely holds temperatures below 2 °C by 2100 (~ 1.96 °C by 2100). In the case of the 2.5% and 3% discount rates, CO₂ concentrations rise before falling as emissions cease. The 2.5% (3%, resp.) discount rate individual also tends to lose ~1% (~1.4%, resp.) more GDP in 2100 and ~1.3% (~2%, resp.) more in 2200 than in the 2% discount rate case, showing the expensive consequences of delayed action in combating climate change.

From this analysis, we find that modeling the cost of climate risk with CAP6 strongly supports stringent mitigation action. We find that the carbon price and corresponding mitigation policy associated with the 2% discount rate saves at least 22 trillion 2020 \$USD globally in 2100 (assuming global GDP grows annually by 4%) in comparison to the higher discount rate policies. In addition, employing policies in line with the 2% discount rate lead to an expected warming in line with the targets laid out in the Paris Agreement, thus avoiding any significant economic and ecological disruptions that become much more likely to occur once the 1.5 °C warming threshold is passed [5, 37]. In the face of potentially catastrophic damages, the representative agent makes a clear choice: they sacrifice consumption today

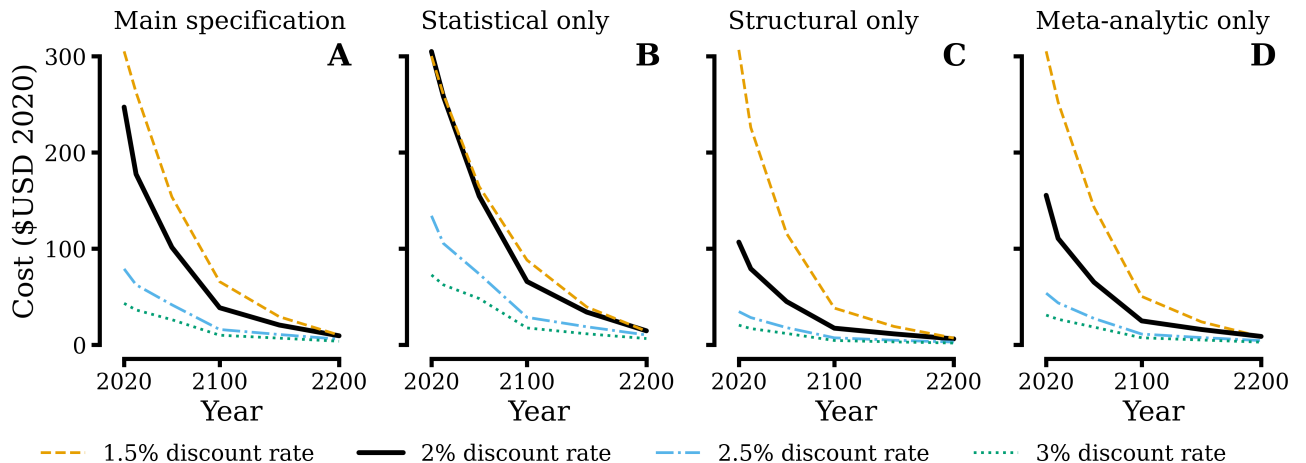


Figure 6: Isolating damage function impact on price paths. Panel **A** shows paths with all damage functions sampled, i.e., our main specification. Panel **B–D** show our featured price paths with a single damage function specified; statistical, structural, and meta-analytic in turn.

to abate CO₂ emissions, rather than test their luck by delaying action, hoping climate damages never arise. Indeed, to this individual, climate change is very much *not* a casino.

3.1.1 Isolating sources of climate-economic risk

We isolate sources of climate-economic risk in Figure 6 by isolating a single damage function and re-running our preferred and featured model runs. For comparison, we also provide our featured runs in panel 6A. Beginning with the statistically estimated damage function, we find that prices are higher in the near term in comparison to the other damage functions, with the exception of the 1.5% discount rate run. This can be explained by the statistically estimated damage function implying higher damages in the long term in comparison to the structural or meta-analytic damage function, thus leading to immediate mitigation action and higher prices so as to avoid catastrophe. Put differently, the probability of low damages is far lower when only the statistical damage function is considered, in comparison to when all three damage functions are considered and weighted as equally probable (as is done in the “main specification” runs).

By comparison, running CAP6 with a convex damage function (i.e., the structural and meta-analytic damage functions) results in lower prices in the near term, with the exception of the 1.5% discount rate runs. This can be attributed to the low damages associated with moderate temperature increase. There is also a significant difference in the level of CO₂ price between the structurally estimated and the meta-analytic damage function for a given discount rate, owing to the difference in the level and acceleration rate of damages assumed in each.

Two crucial insights that can be made from our risk decomposition. The first is that, for sufficiently low discount rates, CAP6 implies stringent mitigation strategies *independent* of damage function shape and scale. This is to say that, for individuals who place a sufficiently high value on future economic utility, any degree of risk associate with high climate damages is worth hedging against. This highlights not only how individual preferences shape preferred policies, but also how they can supersede the details

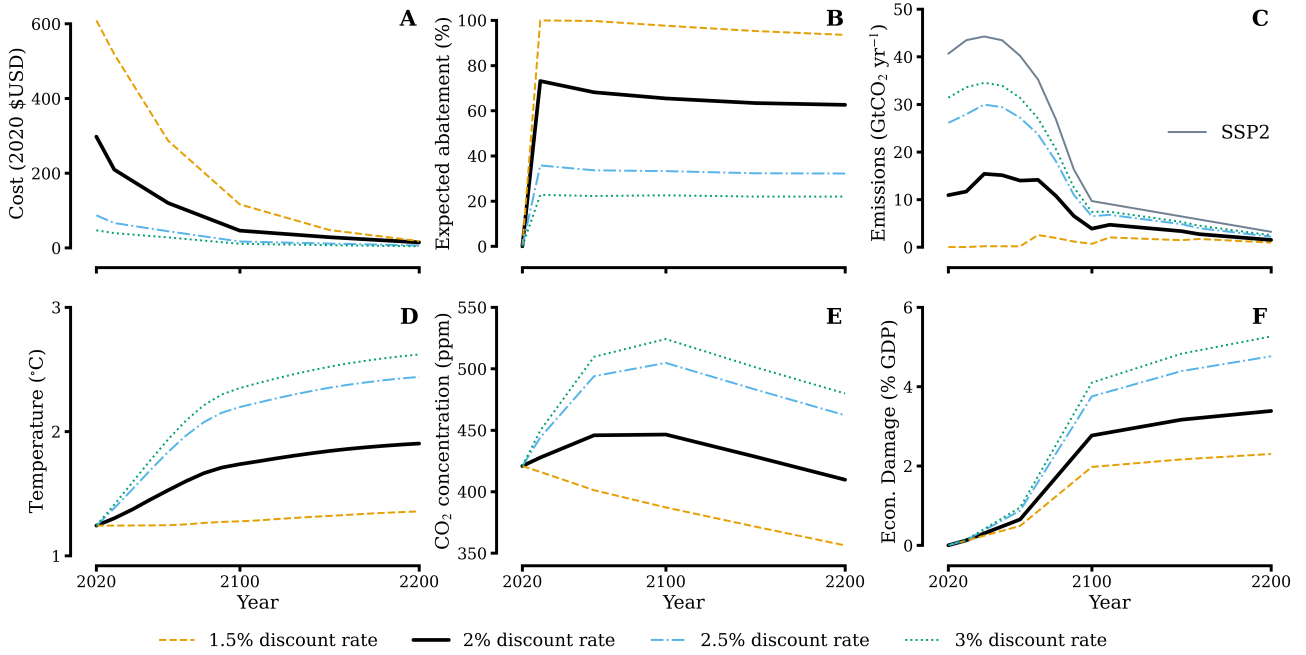


Figure 7: Preferred and featured model runs with “no free lunches” cost curve. We show model output for four discount rates using the “no free lunches” cost curve calibration: 1.5%, 2% (preferred), 2.5%, and 3%. Panels are ordered as in Figure 5.

of the underlying model components. Indeed, risk is truly in the eye of the beholder.

The second insight from this exercise is that the statistical damage function has an outsized impact on the “main specification” price paths (panel 6A) than the other damage functions. This owes to the significantly larger damages that can arise from the statistically estimated damage function, particularly in the long term. These high values present the most catastrophic long-term risks from climate change. Given that our model allows individuals to ‘hedge’ against high climate damages, it stands to reason that the damage function that is most responsible for catastrophic risk (if only relative to the other damage functions considered) has a larger impact on climate price paths than other damage functions. An alternative way of viewing this result is that the risk landscape of climate change is dominated by the risk of climate change slowing economic growth, a phenomenon captured by the statistically estimated damage function. Our findings therefore support the view that the risk of climate change slowing economic growth warrants stringent mitigation strategies [71].

3.2 Alternative calibrations

3.2.1 “No free lunches” calibration

We re-run our preferred and featured runs using the “no free lunches” MACC and show the results in Figure 7. With the exception of the 1.5% discount rate result, the “no free lunches” cost curve does not change the ‘optimal’ price of carbon by a significant amount; the 2020 CO₂ price increases by just \$50 in the 2% discount rate case, a 20% increase. It does, however, change the efficiency of the ‘optimal’ price in abating CO₂ emissions. For example, the 2% discount rate policy now abates only

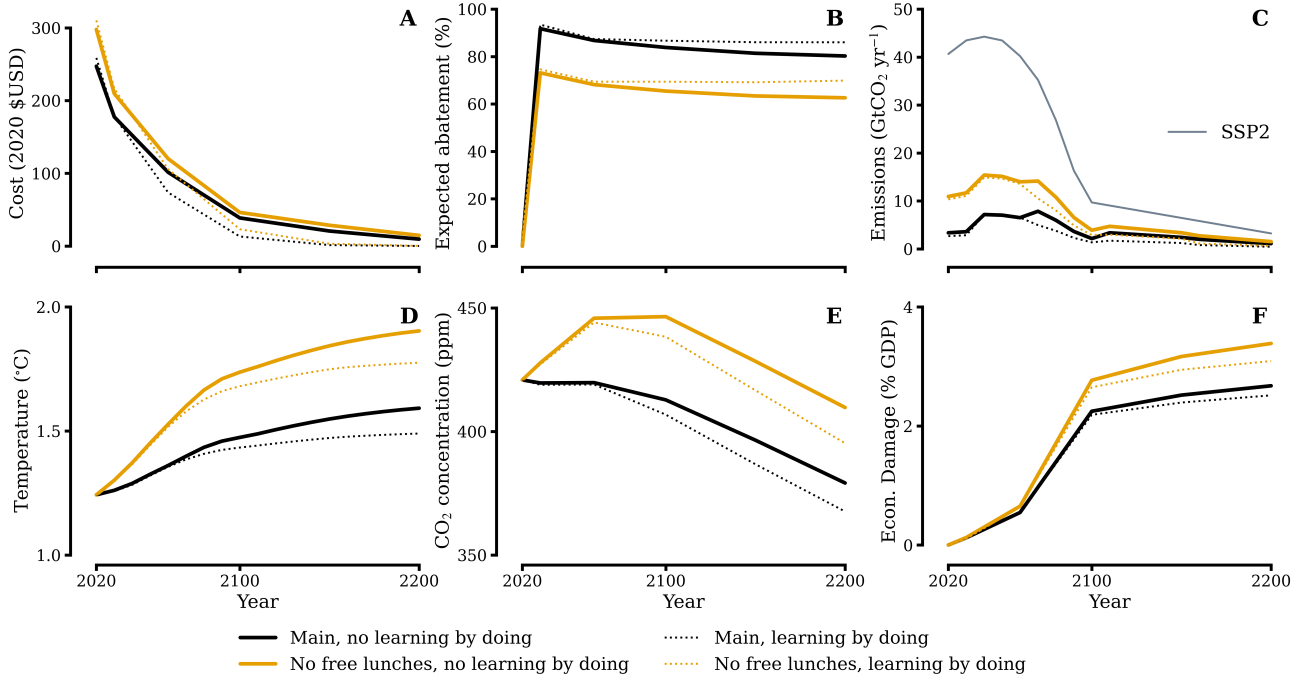


Figure 8: Preferred model runs with “learning by doing” enabled. We show model output using our preferred 2% discount rate and toggling which MACC we use (“main” or “no free lunches”) with or without “learning by doing.” Note that “learning by doing” is enabled if $\varphi_1 = 1.5\%$; no “learning by doing” corresponds to $\varphi_1 = 0\%$. All other parameters are the same as in our main specification. Panels are ordered as in Figure 5.

70% of emissions (as opposed to $\sim 85\%$ in the main specification). This emissions pathway fails to meet the 1.5°C warming target set in the Paris agreement, reaching $\sim 1.7^\circ\text{C}$ warming by 2100 and $\sim 1.9^\circ\text{C}$ warming by 2200, but still maintains less than 2°C warming. This shows that even if the cost of abatement is considerably higher than the IPCC foretells, keeping total warming “well below” 2°C is still ‘optimal’ within CAP6 when a 2% discount rate is used.

Running CAP6 with the “no free lunches” calibration and a 2.5% or 3% discount rates show similar results as the 2% rate: similar ‘optimal’ costs of carbon that correspond to less abatement, more warming, more damages, and higher CO₂ concentrations. In this case, however, we find that using a 2.5% or 3% discount rate exceeds 2°C warming in 2100, thus exceeding the upper bound of allowable warming established in the Paris agreement. This shows that if abatement turns out to be more costly than we expect – owing to the “energy paradox” [48, 3], for example – then using a higher discount rate in climate policy makes the world’s ability of achieving the warming targets in the Paris agreement far more tenuous.

The only exception to the pattern above – similar costs leading to less abatement and more warming – is the 1.5% discount rate policy, which still abates nearly 100% of emissions in the near term. This can be explained by this agent having a remarkably low risk tolerance, and therefore sacrifices considerable consumption to minimize both experienced and potential future damages owing to climate change.

3.2.2 “Learning by doing” demonstration

We run CAP6 with “learning by doing” (i.e., endogenous technological growth) included for both our main specification and “no free lunches” MACC in Figure 8. Note we use a 2% discount rate for each curve in Figure 8 and all other calibration parameters are the same as in our ‘main specification’ runs above. We find that including “learning by doing” does not change the present-day carbon price significantly for either MACC, but it does lower the overall cost burden of the ‘optimal’ abatement policy (i.e., the integrated cost over time). This is owed to prices declining faster as consumption is spent on mitigation, thus enabling more abatement in the near-term for cheaper costs. Furthermore, enabling “learning by doing” lowers the expected ‘optimal’ warming by ~ 0.05 °C in 2100 for both MACCs. For the ‘main specification’ MACC, warming in 2200 is lower by ~ 0.1 °C, whereas for the “no free lunches” MACC 2200 warming is lower by ~ 0.12 °C.

A notable result from this exercise is that by including “learning by doing,” the 2% discount rate policy with our ‘main specification’ cost curve stays below the 1.5 °C warming target in 2200; recall this threshold was exceeded when “learning by doing” was excluded. Hence, we can expect that the feasibility of reaching the warming targets set forth in Paris are highly sensitive to such calibration choices; given that the rate of overall endogenous technological change is difficult to calibrate empirically, this represents a source of uncertainty in policy projections.

3.3 Ensemble model analysis

We probe the influence of uncertainty in model parameters on CO₂ price paths, temperature change, CO₂ concentrations, and economic damages incurred in our ensemble runs, shown in Figure 9. We find that CO₂ price paths decline over time, regardless of socio-economic specification. This is because, regardless of the exogenous emissions baseline we assume, significant climate damages are always possible owing to uncertainties in climate damage functions and TCRE. Therefore, agents mitigate emissions in the near term to rule out the catastrophic futures as they are responding to qualitatively similar risk landscapes, albeit with different absolute levels of the risk (i.e., the amount of potential damages). The level of CO₂ price varies between baselines because the MACC is baseline dependent (see Eqn. (2.16)); for the same fraction of emissions abated, agents pay different prices depending on the baseline. Moreover, each baseline assumes some amount of mitigation, and CAP6 determines the additional price that results in an ‘optimal’ level of warming. This leads to lower emissions baselines having lower prices. Finally, cost variance is highly stratified across baseline, see panel 9F.

Central estimates of temperature, CO₂ concentrations, and economic damages, however, do not see significant differences in central estimates across baselines as was observed in CO₂ prices. This owes to suggested policy in CAP6 being consistent across baselines; the only difference is the price of implementing said policy. Hence, the “impact variables” of temperature change, CO₂ concentrations, and economic damages are relatively insensitive to baseline choice. This is a notable result, as it implies CAP6 finds an ‘optimal’ temperature level across emissions baselines. The variance in each, displayed in panels 9L,R,X, however, are sensitive to the choice in baseline, with high (low, resp.) emissions scenarios having the highest (lowest, resp.) amount of variance. This can be explained by considering the consequences of inaction (i.e., high discount rate policies). In a high emissions scenario such as

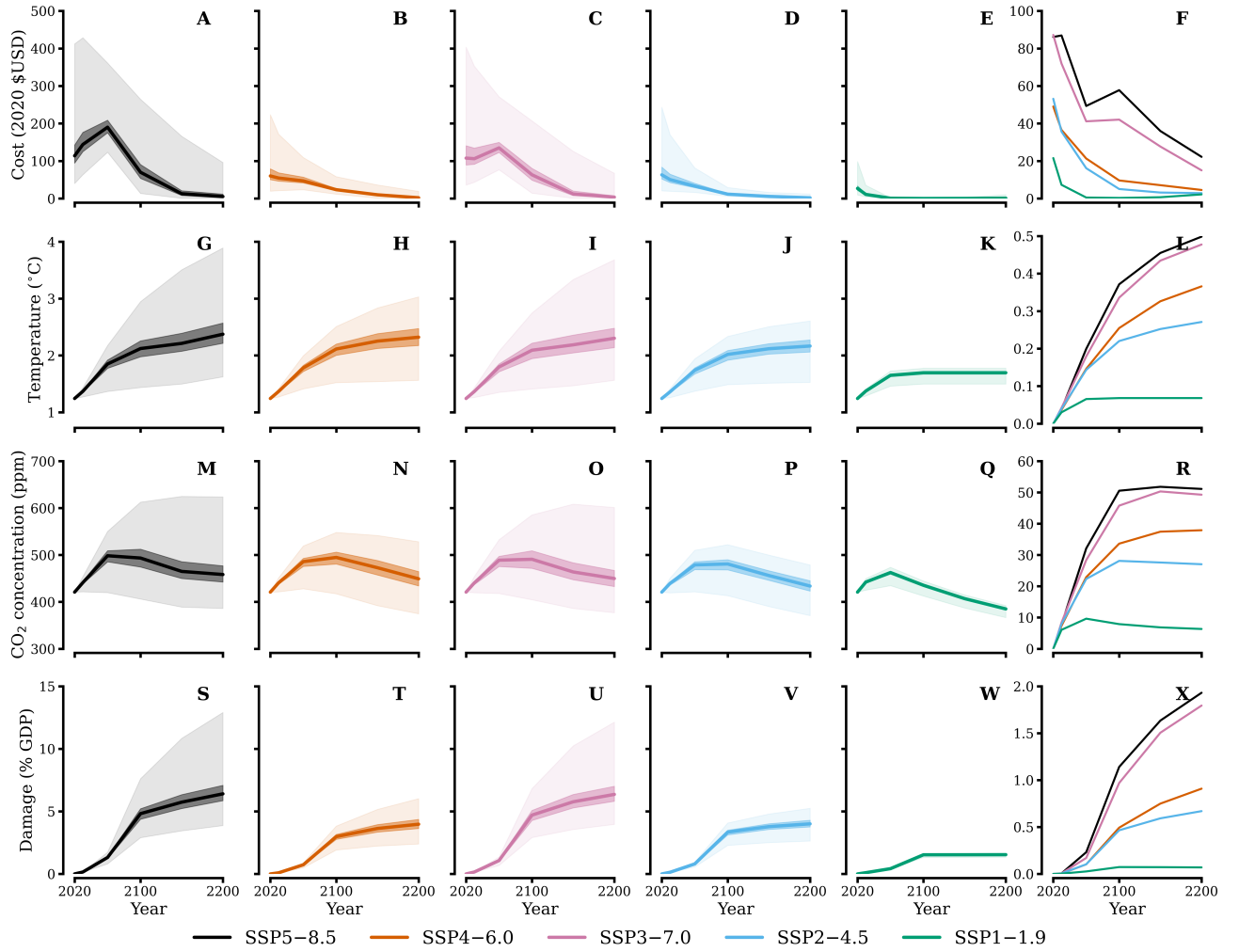


Figure 9: Ensemble model results. We plot the median cost (top row, panels **A–E**), temperature (second from top, panels **G–K**), CO₂ concentrations (third from top, panels **M–Q**), and economic damages (bottom row, panels **S–W**) from our ensemble model runs. In each panel, the dark (light, resp.) shaded region represents the 36th–64th (1st–99th, resp.) percentile range, and the solid lines represent the median time series. In the final column (panels **F**, **L**, **R**, and **X**) we plot the standard deviation of each parameter distribution.

SSP5–8.5, inaction leads to more emissions, and thus warming, atmospheric CO₂, and damages, than in a low emissions scenario such as SSP2–4.5. Hence, the variance in temperature, atmospheric CO₂ concentrations, and economic damages are all higher for high emissions scenarios than in low emissions scenarios.

A final note on the ensemble runs pertains to the level of expected warming, shown in panels 9G–K. Even after sampling a variety of discount rates, levels of risk aversion, rates technological change, and emissions baselines, we find that the median amount of expected warming is approximately 2 °C in 2100 *in each baseline*. The uncertainty in such estimates is, again, baseline dependent, but it is rather remarkable that the expected warming is robustly supportive of the upper bound of acceptable warming established in the Paris agreement [98] even when considering a range of model calibrations.

3.3.1 Variance decomposition of ensemble results

The significant stratification of uncertainty in our output variables shown in Figure 9 motivates further study; is it high discount rates that control prices, for example, or rates of technological change? To this end, we perform a regression analysis of CO₂ price, temperature, CO₂ concentrations, and economic damages at every point in time against parameter values, and plot the fraction of total r^2 attributable to each parameter in Figure 10 (see Appendix B for details on our regression technique and the *Supplementary Information* for supporting figures).

For prices, we find that the discount rate (i.e., EIS and PRTP) dominate uncertainty in the near term (i.e., prior to 2100). This owes to these parameters dictating individual attitudes towards time-related risk and discounting. In early periods of the model, climate damages are highly uncertain (see Figure 1). Therefore, any abatement action that is taken is with the intent to rule out the most catastrophic outcomes and secure future wellbeing; the extent to which individuals respond to this threat of catastrophe is governed by EIS and PRTP, thus determining the level of early mitigation action and driving costs. On longer timescales (past 2100), climate damages have been more distinctly realized, and the number of possible futures have narrowed. Individuals must come to grips with their damaged future, and generally begin investing more stringently in emissions abatement. This comes at a cost, a cost that is higher if they haven't invested in mitigation in earlier decision periods (see Eqn. (2.16)). This uniformity of abatement action explains why technological growth rates dominate prices in the long term; once all individuals decide to solve the problem of climate change, the price of doing so is determined by how much cheaper abatement technologies have become in the time it took to reach this decision. In particular, high prices in late periods are almost entirely attributable to low rates of technological change (which, thankfully, seem increasingly unlikely as time progresses [44, 102, 49, 90, 79, 54, 34]). These findings are robust for every SSP we considered.

For temperature, CO₂ concentrations, and economic damages, however, a different story emerges. The influence of EIS and PRTP is pronounced for much longer than in the case of CO₂ prices. This owes to inactivity early on leading to long-term consequences in the form of temperature rise, more CO₂ in the atmosphere, and economic damage that cannot simply be fixed by more spending on abatement. Indeed, while technological change can certainly halt any further increase in global mean surface temperature, for example, it cannot undo past malfeasance (in the absence of significant negative emissions or solar

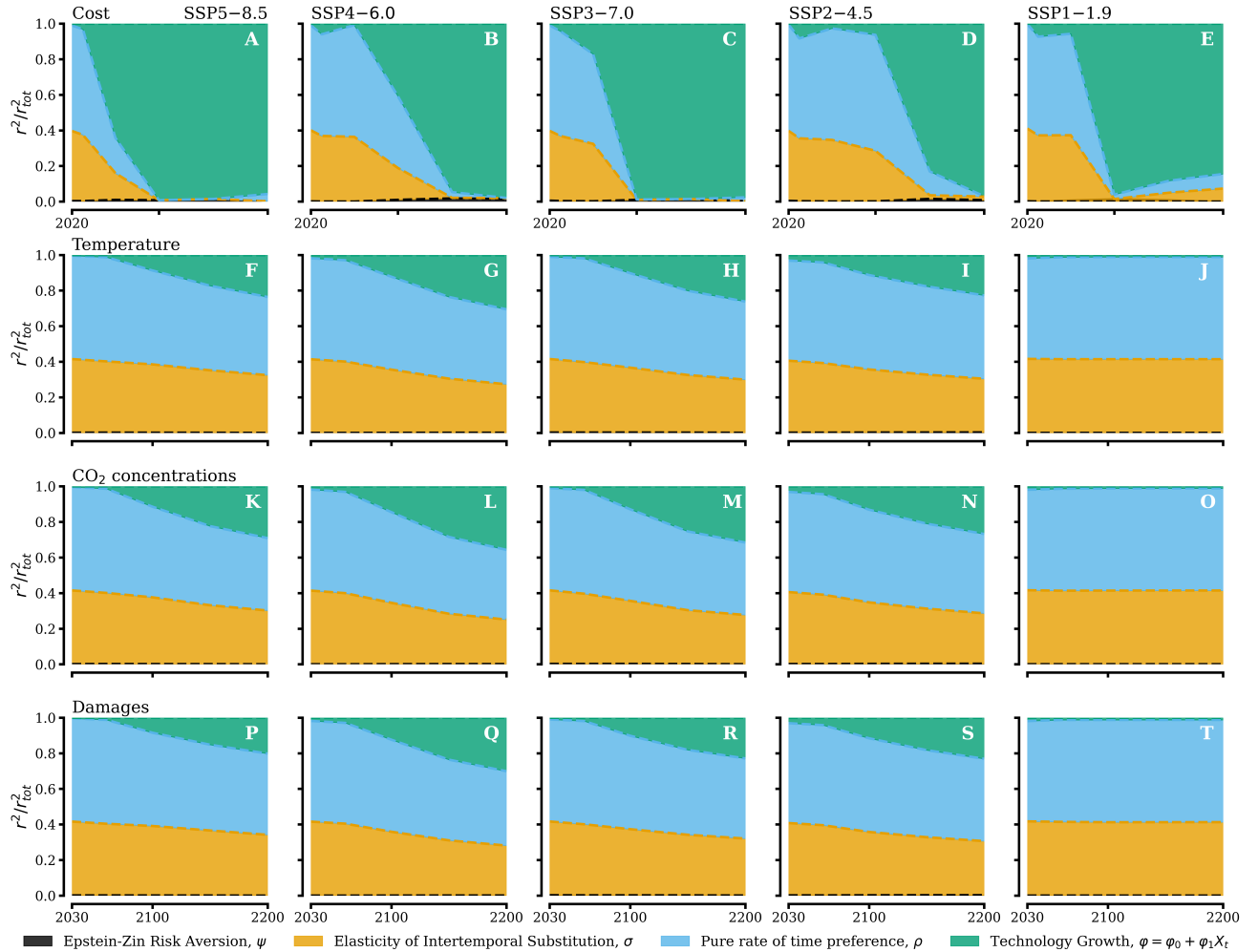


Figure 10: Variance attribution. In each row, we plot the fraction of total variance (calculated as total r^2) attributable to each model parameter for carbon prices (top row, panels **A–E**), temperature (second row, panels **F–J**), CO₂ concentrations (third row, panels **K–O**), and economic damages (bottom row, panels **P–T**). Each column represents a different SSP. Note that cost variance (top row) begins in 2020 whereas temperature, CO₂ concentrations, and economic damages (bottom three rows) begin in 2030, as the model is initialized with the same climate conditions and no damages incurred, leading to zero variance in 2020 for the latter three variables.

geoengineering [46, 36, 67], an important qualification to this conclusion). Hence, EIS and PRTP have a much more pronounced influence on far-distant temperature rise, atmospheric CO₂ levels, and economic damages than in the case of CO₂ prices.

Interestingly, Figure 10 shows that agent RA (i.e., the value of ψ) is irrelevant for carbon price, temperature, CO₂ concentrations, or damage uncertainty. (This is not to say that RA has no impact on price levels, as increasing (decreasing, resp.) RA does slightly raise (lower, resp.) near term prices (see the *Supplementary Information*).) This is a surprising, though not necessarily new, result [2]; given the inherently probabilistic nature of climate change, and the very real possibility of catastrophe [55], it stands to reason that individual aversion to risk would play a major role in CO₂ abatement policy.

There are two potential explanations for this finding. The first is related to our MACC being totally unambiguous throughout time. This implies that an agent always understands that he *can* solve the problem of climate change, for some amount of money, and just *chooses* not to, depending on his preference towards sacrificing consumption (i.e., his EIS). This implies that solving climate change in the context of CAP6 is a matter of optimizing *when* to dedicate available resources to abatement, which is why prices are strongly tied to discounting parameters (EIS and PRTP) rather than RA. Put differently, the risk landscape presented in CAP6 is incomplete; not only should risk associated with damages factor into decision making, but also the risk of a lack of technological ability should also be considered, and is not currently in CAP6.

A second explanation for risk aversion (in the Epstein-Zin sense of risk aversion across states of nature, captured by ψ) being of little importance for long-term climate policy is that, owing to the large residence time of CO₂ in the atmosphere and the large time horizons for incurring economic damages, the impact of risk aversion with respect to time swamps the impact of risk aversion across states of nature. Indeed, the results of Figure 10 provide resounding support for this theory: risk aversion across states of time (captured by EIS) completely drown out the influence of risk across states of nature (as captured by RA). More work is needed to fully understand how — if at all — risk aversion across states of nature is relevant for climate policy, and how it would alter the results we have presented here.

4 Discussion

4.1 Key findings

OUR work builds on three decades of work in the climate-economic literature, merging it with insights from the financial modeling literature that have largely been developed in parallel [60]. Equally important, the Carbon Asset Pricing model – AR6 (CAP6) is fully up-to-date with the findings of the IPCC’s latest assessment report, AR6 [42, 43, 44]. CO₂ emissions are mapped to temperature via a transient climate response to emissions approach, damage functions are sampled through a variety of estimation techniques, marginal damages from climate tipping points are included, and our marginal abatement cost curve is calibrated to empirical data. We calibrate CAP6 to recent empirical work on the US bond market [99], using a 2% discount rate as our preferred rate [75].

We find that the policies derived from the preferred calibration of CAP6 support stringent mitigation of CO₂ emissions ($\sim 85\%$ abatement in the long term, see Figure 5). The cost of carbon is high in the near

term and declines over time, as mitigation technology becomes increasingly affordable. Furthermore, the implied expected warming level is below the 1.5 °C warming in 2100 target set forth in the Paris agreement. To our knowledge, this is the first study that provides economic support for the warming targets set forth in Paris without any additional normative calibrations or judgements.

The stringent mitigation policy suggested in the preferred run of CAP6 can be traced back to risk associated with climate change slowing economic growth, thus leading to high damages in the long term (see Figure 6). This corroborates other work that the risk of slowed growth should lead to strict CO₂ abatement policies [71]. For sufficiently low discount rates, however, we find that individual preferences trump the details of the damage function, and any degree of damages from climate change are mitigated against. This showcases not just how individual preferences can influence policy choices, but also how they can supersede the details of the model components to dominate policy recommendations.

In addition to our ‘main specification,’ we provide two alternative calibrations of CAP6. First, we run CAP6 assuming the cost of abating CO₂ emissions is much higher than AR6 estimates (coining this the “no free lunches” calibration), and show the results in Figure 7. We find that even when assuming the cost of abating CO₂ is much higher than the data presented in the AR6 – perhaps owing to the “energy paradox” [48, 3] – using a 2% discount rate still results in abatement policy with expected ‘optimal’ warming below the 2 °C warming maximum in the Paris agreement (~ 1.7 °C in 2100, ~ 1.8 °C in 2200). However, the feasibility of staying beneath the 2 °C maximum depends on the discount rate specified; ‘optimal’ policy associated with the “no free lunches” MACC and a 2.5% or 3% discount rate exceeds 2 °C by 2100, and approaches 2.5 °C of warming by 2200. This highlights that if indeed the cost of abatement is severely underestimated by the IPCC, aggressive emissions mitigation policy (via a high carbon price) is required to meet the warming targets in the Paris agreement.

The second alternative calibration is with “learning by doing” (i.e., endogenous technological change) enabled. We find that including this effect results in little change in present-day carbon prices, regardless of which MACC we assume (i.e., our ‘main’ MACC or the “no free lunches” MACC). However, we do find that, in the long-term, “learning by doing” results in lower warming levels, as large up-front investment made in the early decision periods of CAP6 (as demonstrated by high near-term prices) lead to lower abatement costs and thus more deployment. Quantitatively, “learning by doing” lowers 2200 warming by ~ 0.1 °C in each MACC we considered, assuming a 2% discount rate.

To understand how the discount rate and technological growth rates influence CAP6 model output, we sample a range of model parameters in our ensemble runs (see Figure 9). We find that central estimates of CO₂ price are sensitive to the choice of baseline. This owes to our marginal abatement cost curve being baseline dependent, which in turn modulates the amount of consumption required to abate the same fraction of emissions in different baselines. Central estimates of temperature change, CO₂ concentrations, and economic damages, on the other hand, are robust to baseline choices, as the suggested policy in CAP6 is relatively consistent across baselines, thus leading to similar outcomes in these variables. This finding is notable, as it implies CAP6 captures the differences in mitigation assumed in each baseline and solves for a robust ‘optimal’ level of warming regardless of the baseline assumed. Moreover, the median warming in our ensemble runs is approximately 2 °C in 2100, providing yet more support for the warming targets set forth in the Paris agreement.

We find that the uncertainty in CAP6 ensemble output is highly stratified by emissions baseline. We

decompose output variance and attribute uncertainty to different socio-economic parameters, highlighting in particular the time-dependency of parameter influence on output uncertainty (Figure 10). In particular, we find that prices in the near term are dominated by discounting parameters, while in the long term, technological growth controls carbon prices. For temperature, CO₂ concentrations, and economic damages, however, we find that discounting parameters influence uncertainty for much longer than in the case of prices. This can be explained by the result of early inactivity; inactivity leads to temperature change, increased CO₂ in the atmosphere, and economic damage that cannot be undone by spending more on abatement (in the absence of any significant negative emissions or solar geoengineering).

Nearly 10 years ago, Lord Nicholas Stern wrote, “presenting the [climate] problem as risk-management is likely to point strongly towards a policy for a rapid transition to a low-carbon economy” [93]. Our framework takes this view seriously, and, in the final analysis, highlights the wisdom in Stern’s words. Indeed, by treating CO₂ as a risky asset and calculating the ‘optimal’ CO₂ price and associated abatement policy, we find that ‘optimal’ policy limits warming below 2 °C even if we are pessimistic about cost of abatement estimates provided by the IPCC; taking the optimistic view on costs results in a policy with less than 1.5 °C of warming in 2100, in line with the target set forth in the Paris agreement. Practically speaking, this corresponds to cutting $\gtrsim 60\%$ of CO₂ emissions in relatively short order; a “rapid transition to a low-carbon economy” indeed. Our results therefore flip the conventional view of climate policy on its head; rather than abating progressively more CO₂ emissions as time goes on (and damages are felt more acutely), our model suggests more stringent early abatement as a ‘hedge’ against the potentially catastrophic damages presented by climate change.

4.2 Limitations and directions for future work

Our work has a number of limitations that open more directions for future work. A major qualification to our results regards our cost of CO₂ abatement. The first major assumption is that abatement technologies are essentially instantly able to be deployed; we do not capture real-world inertia, represented in other energy systems IAMs, that cap the rate of decarbonization owing to the delayed availability of abatement technologies, stranded assets, limited construction times, and other factors [32, 86]. Moreover, our MACC assumes that the sacrificed consumption to abate CO₂ emissions does not feedback on other aspects of the economy, such as growth or productivity [38]. The scope of this paper was to explore the influence climate-related risk assessment and how this influences carbon pricing, but including the feedback of mitigation policy on growth would be an interesting direction for future work. These limitations provide important context for the ‘optimality’ of our results; they should not be over-interpreted to imply that the institution of such a policy would necessarily be the most economically efficient.

A second route to improve the results discussed here is to allow for stochastic, growth-rate dependent discounting, which would improve on CAP6’s static discounting assumption. Implementing these modules into CAP6 would lead to a more accurate economic model and representation of agent attitudes towards the future. Moreover, this would allow for the known link between damages and growth to be explicitly established, which generally lowers the estimates of the SCC [75].

Another improvement is to allow mitigation action to feedback on the emissions baseline, and thus, agent risk assessment. In the current version, CAP6 is always considering the risk posed by the full SSP, but in reality, once some amount of emissions are abated, the level of risk should change in turn. Moreover, if technology in dirty sectors is phased out in favor of renewables, dirty energy at the scale of the original baseline should be unavailable to agents. This, however, is not the case in CAP6. Agents always have the option to emit CO₂ at the scale of the original baseline; so to speak, they can always “turn the coal plants back on” for no additional cost. Allowing for this mitigation action-emissions baseline feedback would improve the work here, and would likely lower cost estimates in the long term, owing to less risk after abating stringently early on.

A final topic for future work arises out of our variance decomposition (i.e., Figure 10): agent risk aversion with respect to states of nature has a negligible influence on price, temperature, CO₂ concentrations, and economic damage uncertainty. Given the inherently uncertain nature of climate change and its impacts, it is surprising that this dimension of risk aversion would matter so little. More work is needed to determine if it is indeed the case that risk aversion across states of nature is truly irrelevant in comparison to risk across time for climate policy, or if the model presented here is simply ill-equipped to capture its role fully.

A Damage function calibration

We fit the damage function data in the following way. For each damage function, we require that the concavity of the damage function is preserved, i.e., $\partial^2\mathcal{D}/\partial T'^2 \geq 0$, depending on the damage function being considered. To solve for the damage function coefficients as presented in (2.6), we require knowing the damages for two data points, generically labeled as (T_1, \mathcal{D}_1) and (T_2, \mathcal{D}_2) . Then we can write

$$\mathcal{D}_1 = T_1(\varpi_2 T_1 + \varpi_1), \quad (\text{A.1})$$

$$\mathcal{D}_2 = T_2(\varpi_2 T_2 + \varpi_1), \quad (\text{A.2})$$

and, solving the above for ϖ_1 and ϖ_2 , results in

$$\varpi_1 = \frac{\mathcal{D}_1 T_2^2 - \mathcal{D}_2 T_1^2}{T_2 T_1 (T_2 - T_1)}, \quad (\text{A.3})$$

$$\varpi_2 = \frac{\mathcal{D}_2 T_1 - \mathcal{D}_1 T_2}{T_2 T_1 (T_2 - T_1)}. \quad (\text{A.4})$$

Having established the mean state, we can now introduce uncertainty into (A.3) and (A.4). We do so by allowing \mathcal{D}_1 to be uncertain, assigning it a Gaussian distribution $\tilde{\mathcal{D}}_1$ with mean $\bar{\mathcal{D}}_1$ and standard deviation $\sigma_{\mathcal{D}_1}$. We link this to a distribution of \mathcal{D}_2 by invoking the condition $\partial^2\mathcal{D}/\partial T'^2 \geq 0$, immediately resulting in the condition $\varpi_2 \geq 0$. Using (A.4), we arrive at

$$\tilde{\mathcal{D}}_2 \geq \tilde{\mathcal{D}}_1 \left(\frac{T_2}{T_1} \right). \quad (\text{A.5})$$

Eqn. (A.5) is generic for any damage function, but our model, we want either a concave up or concave down damage function. To accomplish this, we include an additional factor $\Lambda > 0$ to (A.5) such that

Table 6: Damage function calibration values. Fitted parameters for the damage function calibration equation (A.6) based on [43] and [20].

Damage function	$\bar{\mathcal{D}}_1 [-]$	$\sigma_{\mathcal{D}_1} [-]$	Λ
Statistically estimated [8]			
SSP1, mid-century	0.075	0.01	2.5
SSP2, mid-century	0.065	0.01	2.0
SSP3, mid-century	0.062	0.01	2.0
SSP4, mid-century	0.049	0.01	2.5
SSP5, mid-century	0.065	0.01	2.1
SSP1, end-of-century	0.2	0.04	0.87
SSP2, end-of-century	0.195	0.04	0.75
SSP3, end-of-century	0.19	0.04	0.69
SSP4, end-of-century	0.13	0.04	0.82
SSP5, end-of-century	0.155	0.04	0.82
Structurally estimated [89, 95]	0.027	0.01	2.8
Meta analysis of climate damages [41]	0.063	0.022	3.3

the inequality is ensured, i.e.,

$$\tilde{\mathcal{D}}_2 = \Lambda \tilde{\mathcal{D}}_1 \left(\frac{T_2}{T_1} \right), \quad \text{such that } \Lambda \gtrless 1. \quad (\text{A.6})$$

Therefore, if $\Lambda > 1$, we have a concave up damage function, and if $\Lambda < 1$, we have a concave down damage function. Setting $T_1 = 3$ °C and $T_2 = 10$ °C, we fit values for $\bar{\mathcal{D}}_1$, $\sigma_{\mathcal{D}_1}$, and Λ to each set of damage function data resulting in the values presented in Table 1. See Table 6 for the values of our calibration coefficients.

B Regression analysis

Regression coefficients in Figure 10 are calculated by fitting a linear regression between each parameter value and carbon costs. The one exception is technological growth, which is time dependent and given by

$$\varphi := \varphi_0 + \varphi_1 X_t. \quad (\text{B.1})$$

In 2100 and later, technological change is clearly nonlinearly related to carbon costs (see the *Supplementary Information*). We therefore fit a quadratic to carbon costs as a function of total technological growth from 2100 on. Costs increase in some cases when technological growth is remarkably high, owing to the deployment of additional negative emissions technologies.

Acknowledgments

The code for the Carbon Asset Pricing model – AR6 can be found [here](#). Some computational components of the Carbon Asset Pricing model – AR6 are taken from [EZClimate](#), a financial asset pricing climate-economy model developed by Kent D. Daniel, Robert B. Litterman, and Gernot Wagner. Time series for CO₂ emissions are taken from the [SSP database](#). The concentration of carbon dioxide currently in the atmosphere is owed to the [Scripps Institution of Oceanography's Keeling curve program](#). The authors thank Romain Fillon, Bob Kopp, Bob Litterman, James Rising, Chris Smith, Thomas Stoerk, and Andrew Wilson for providing feedback on the manuscript. The authors kindly thank Alaa Al Khourdajie for providing the data from AR6 WGIII's marginal abatement cost figure. The authors thank W. Matthew Alampay Davis and Steve Rose for helpful discussions regarding climate damage functions. The authors thank David C. Lafferty for his contributions to Figure 6 and to Jaydeep Pillai for testing the public release version of the code. AMB thanks Columbia Business School for their hospitality while this work was being completed. AMB acknowledges support from the Gies College of Business Office of Risk Management and Insurance at the University of Illinois at Urbana Champaign, Columbia Business School, and a National Science Foundation Graduate Research Fellowship grant No. DGE 21-46756. CP was supported by the Gies College of Business Office of Risk Management and Insurance at the University of Illinois at Urbana Champaign. Computations were performed on the Keeling computing cluster, a computing resource operated by the School of Earth, Society and the Environment (SESE) at the University of Illinois at Urbana Champaign.

References

- [1] D. ACEMOGLU, P. AGHION, L. BURSZTYN, AND D. HEMOUS, *The Environment and Directed Technical Change*, American Economic Review, 102 (2012), pp. 131–166.
- [2] F. ACKERMAN, E. A. STANTON, AND R. BUENO, *Epstein-Zin Utility in DICE: Is Risk Aversion Irrelevant to Climate Policy?*, Environmental and Resource Economics, 56 (2013), pp. 73–84.
- [3] H. ALLCOTT AND D. TAUBINSKY, *Evaluating Behaviorally Motivated Policy: Experimental Evidence from the Lightbulb Market*, American Economic Review, 105 (2015), pp. 2501–2538.
- [4] M. R. ALLEN, D. J. FRAME, C. HUNTINGFORD, C. D. JONES, J. A. LOWE, M. MEINSHAUSEN, AND N. MEINSHAUSEN, *Warming caused by cumulative carbon emissions towards the trillionth tonne*, Nature, 458 (2009), pp. 1163–1166.
- [5] D. I. ARMSTRONG MCKAY, A. STAAL, J. F. ABRAMS, R. WINKELMANN, B. SAKSCHEWSKI, S. LORIANI, I. FETZER, S. E. CORNELL, J. ROCKSTRÖM, AND T. M. LENTON, *Exceeding 1.5°C global warming could trigger multiple climate tipping points*, Science, 377 (2022), p. eabn7950.
- [6] M. BARNETT, W. BROCK, AND L. P. HANSEN, *Pricing Uncertainty Induced by Climate Change*, The Review of Financial Studies, 33 (2020), pp. 1024–1066.
- [7] B. BOLLINGER AND K. GILLINGHAM, *Learning-by-Doing in Solar Photovoltaic Installations*, Feb. 2019.

- [8] M. BURKE, W. M. DAVIS, AND N. S. DIFFENBAUGH, *Large potential reduction in economic damages under UN mitigation targets*, Nature, 557 (2018), pp. 549–553.
- [9] M. BURKE, S. M. HSIANG, AND E. MIGUEL, *Global non-linear effect of temperature on economic production*, Nature, 527 (2015), pp. 235–239.
- [10] Y. CAI AND T. S. LONTZEK, *The Social Cost of Carbon with Economic and Climate Risks*, Journal of Political Economy, 127 (2019), pp. 2684–2734.
- [11] K. CALVIN, B. BOND-LAMBERTY, L. CLARKE, J. EDMONDS, J. EOM, C. HARTIN, S. KIM, P. KYLE, R. LINK, R. MOSS, H. MCJEON, P. PATEL, S. SMITH, S. WALDHOFF, AND M. WISE, *The SSP4: A world of deepening inequality*, Global Environmental Change, 42 (2017), pp. 284–296.
- [12] T. A. CARLETON AND S. M. HSIANG, *Social and economic impacts of climate*, Science, 353 (2016), p. aad9837.
- [13] T. F. COLEMAN, N. S. DUMONT, W. LI, W. LIU, AND A. RUBTSOV, *Optimal Pricing of Climate Risk*, Computational Economics, (2021).
- [14] COMMITTEE ON ASSESSING APPROACHES TO UPDATING THE SOCIAL COST OF CARBON, BOARD ON ENVIRONMENTAL CHANGE AND SOCIETY, DIVISION OF BEHAVIORAL AND SOCIAL SCIENCES AND EDUCATION, AND NATIONAL ACADEMIES OF SCIENCES, ENGINEERING, AND MEDICINE, *Valuing Climate Changes: Updating Estimation of the Social Cost of Carbon Dioxide*, National Academies Press, Washington, D.C., 2017.
- [15] COUNCIL OF ECONOMIC ADVISORS, *Discounting for public policy: Theory and recent evidence on the merits of updating the discount rate*, tech. rep., Washington, DC, 2017.
- [16] J. C. COX, S. A. ROSS, AND M. RUBINSTEIN, *Option pricing: A simplified approach*, Journal of Financial Economics, 7 (1979), pp. 229–263.
- [17] H. DAMON MATTHEWS, K. B. TOKARSKA, J. ROGELJ, C. J. SMITH, A. H. MACDOUGALL, K. HAUSTEIN, N. MENGIS, S. SIPPEL, P. M. FORSTER, AND R. KNUTTI, *An integrated approach to quantifying uncertainties in the remaining carbon budget*, Communications Earth & Environment, 2 (2021), p. 7.
- [18] K. DANIEL, R. LITTERMAN, AND G. WAGNER, *Applying Asset Pricing Theory to Calibrate the Price of Climate Risk*, Tech. Rep. w22795, National Bureau of Economic Research, Cambridge, MA, Nov. 2016.
- [19] K. D. DANIEL, R. B. LITTERMAN, AND G. WAGNER, *Declining CO₂ price paths*, Proceedings of the National Academy of Sciences, 116 (2019), pp. 20886–20891.
- [20] S. DIETZ, J. RISING, T. STOERK, AND G. WAGNER, *Economic impacts of tipping points in the climate system*, Proceedings of the National Academy of Sciences, 118 (2021), p. e2103081118.

- [21] S. DIETZ, F. VAN DER PLOEG, A. REZAI, AND F. VENMANS, *Are Economists Getting Climate Dynamics Right and Does It Matter?*, Journal of the Association of Environmental and Resource Economists, 8 (2021), pp. 895–921.
- [22] M. A. DRUPP, M. C. FREEMAN, B. GROOM, AND F. NESJE, *Discounting Disentangled*, American Economic Journal: Economic Policy, 10 (2018), pp. 109–134.
- [23] L. G. EPSTEIN AND S. E. ZIN, *Substitution, Risk Aversion, and the Temporal Behavior of Consumption and Asset Returns: A Theoretical Framework*, Econometrica, 57 (1989), p. 937.
- [24] ———, *Substitution, Risk Aversion, and the Temporal Behavior of Consumption and Asset Returns: An Empirical Analysis*, Journal of Political Economy, 99 (1991), pp. 263–286.
- [25] O. FRICKO, P. HAVLIK, J. ROGELJ, Z. KLIMONT, M. GUSTI, N. JOHNSON, P. KOLP, M. STRUBEGGER, H. VALIN, M. AMANN, T. ERMOLIEVA, N. FORSELL, M. HERRERO, C. HEYES, G. KINDERMANN, V. KREY, D. L. MCCOLLUM, M. OBERSTEINER, S. PACHAURI, S. RAO, E. SCHMID, W. SCHOEPP, AND K. RIAHI, *The marker quantification of the Shared Socioeconomic Pathway 2: A middle-of-the-road scenario for the 21st century*, Global Environmental Change, 42 (2017), pp. 251–267.
- [26] S. FUJIMORI, T. HASEGAWA, T. MASUI, K. TAKAHASHI, D. S. HERRAN, H. DAI, Y. HIJOKA, AND M. KAINUMA, *SSP3: AIM implementation of Shared Socioeconomic Pathways*, Global Environmental Change, 42 (2017), pp. 268–283.
- [27] M. J. GIDDEN, K. RIAHI, S. J. SMITH, S. FUJIMORI, G. LUDEKER, E. KRIEGLER, D. P. VAN VUUREN, M. VAN DEN BERG, L. FENG, D. KLEIN, K. CALVIN, J. C. DOELMAN, S. FRANK, O. FRICKO, M. HARMSEN, T. HASEGAWA, P. HAVLIK, J. HILAIRE, R. HOESLY, J. HORING, A. POPP, E. STEHFEST, AND K. TAKAHASHI, *Global emissions pathways under different socioeconomic scenarios for use in CMIP6: a dataset of harmonized emissions trajectories through the end of the century*, Geoscientific Model Development, 12 (2019), pp. 1443–1475.
- [28] N. P. GILLETT, V. K. ARORA, D. MATTHEWS, AND M. R. ALLEN, *Constraining the Ratio of Global Warming to Cumulative CO₂ Emissions Using CMIP5 Simulations**, Journal of Climate, 26 (2013), pp. 6844–6858.
- [29] K. GILLINGHAM AND J. H. STOCK, *The Cost of Reducing Greenhouse Gas Emissions*, Journal of Economic Perspectives, 32 (2018), pp. 53–72.
- [30] D. E. GOLDBERG, *Genetic algorithms in search, optimization, and machine learning*, Addison-Wesley Pub. Co, Reading, Mass, 1989.
- [31] L. H. GOULDER, *Environmental taxation and the double dividend: A reader's guide*, International Tax and Public Finance, 2 (1995), pp. 157–183.
- [32] M. HA-DUONG, M. J. GRUBB, AND J.-C. HOURCADE, *Influence of socioeconomic inertia and uncertainty on optimal CO₂-emission abatement*, Nature, 390 (1997), pp. 270–273.

- [33] M. C. HÄNSEL, M. A. DRUPP, D. J. JOHANSSON, F. NESJE, C. AZAR, M. C. FREEMAN, B. GROOM, AND T. STERNER, *Climate economics support for the UN climate targets*, Nature Climate Change, 10 (2020), pp. 781–789.
- [34] Z. HAUSFATHER AND G. P. PETERS, *Emissions – the ‘business as usual’ story is misleading*, Nature, 577 (2020), pp. 618–620.
- [35] E. HAWKINS AND R. SUTTON, *The Potential to Narrow Uncertainty in Regional Climate Predictions*, Bulletin of the American Meteorological Society, 90 (2009), pp. 1095–1108.
- [36] G. HEUTEL, J. MORENO-CRUZ, AND S. SHAYEGH, *Solar geoengineering, uncertainty, and the price of carbon*, Journal of Environmental Economics and Management, 87 (2018), pp. 24–41.
- [37] O. HOEGH-GULDBERG, D. JACOB, M. BINDI, S. BROWN, I. CAMILLONI, A. DIEDHIOU, R. DJALANTE, K. EBI, F. ENGELBRECHT, J. GUIOT, ET AL., *Global Warming of 1.5°C: IPCC Special Report on impacts of global warming of 1.5°C above pre-industrial levels in context of strengthening response to climate change, sustainable development, and efforts to eradicate poverty*, Cambridge University Press, Cambridge, UK and New York, NY, USA, 1 ed., June 2018.
- [38] W. W. HOGAN AND D. W. JORGENSEN, *Productivity trends and the cost of reducing CO₂ emissions*, The Energy Journal, 12 (1991), pp. 67–85.
- [39] C. HOPE, J. ANDERSON, AND P. WENMAN, *Policy analysis of the greenhouse effect*, Energy Policy, 21 (1993), pp. 327–338.
- [40] K. Z. HOUSE, A. C. BACLIG, M. RANJAN, E. A. VAN NIEROP, J. WILCOX, AND H. J. HERZOG, *Economic and energetic analysis of capturing CO₂ from ambient air*, Proceedings of the National Academy of Sciences, 108 (2011), pp. 20428–20433.
- [41] P. H. HOWARD AND T. STERNER, *Few and Not So Far Between: A Meta-analysis of Climate Damage Estimates*, Environmental and Resource Economics, 68 (2017), pp. 197–225.
- [42] INTERGOVERNMENTAL PANEL ON CLIMATE CHANGE, *Climate change 2021: The physical science basis*, (2021).
- [43] ——, *Climate change 2022: Impacts, adaptation, and vulnerability*, (2022).
- [44] ——, *Climate change 2022: Mitigation of climate change*, (2022).
- [45] INTERNATIONAL ENERGY AGENCY, *Global Energy Review: CO₂ Emissions in 2021*, tech. rep., IEA, Paris, FR, Mar. 2022.
- [46] P. J. IRVINE, B. KRAVITZ, M. G. LAWRENCE, AND H. MURI, *An overview of the Earth system science of solar geoengineering*, WIRES Climate Change, 7 (2016), pp. 815–833.
- [47] A. B. JAFFE, R. G. NEWELL, AND R. N. STAVINS, *A tale of two market failures: Technology and environmental policy*, Ecological Economics, 54 (2005), pp. 164–174.

- [48] A. B. JAFFE AND R. N. STAVINS, *The energy paradox and the diffusion of conservation technology*, Resource and Energy Economics, 16 (1994), pp. 91–122.
- [49] J. JENKINS AND V. KARPLUS, *Carbon pricing under binding political constraints*, WIDER Working Paper Series, Paper 2016 / 44 (2016).
- [50] K. JOHNSON, D. MARTIN, X. ZHANG, C. DEYOUNG, AND A. STOLBERG, *Carbon Dioxide Removal Options: A Literature Review Identifying Carbon Removal Potentials and Costs*, (2017).
- [51] F. JOOS, R. ROTH, J. S. FUGLESTVEDT, G. P. PETERS, I. G. ENTING, W. VON BLOH, V. BROVKIN, E. J. BURKE, M. EBY, N. R. EDWARDS, T. FRIEDRICH, T. L. FRÖLICHER, P. R. HALLORAN, P. B. HOLDEN, C. JONES, T. KLEINEN, F. T. MACKENZIE, K. MATSUMOTO, M. MEINSHAUSEN, G.-K. PLATTNER, A. REISINGER, J. SEGSCHNEIDER, G. SHAFER, M. STEINACHER, K. STRASSMANN, K. TANAKA, A. TIMMERMANN, AND A. J. WEAVER, *Carbon dioxide and climate impulse response functions for the computation of greenhouse gas metrics: a multi-model analysis*, Atmospheric Chemistry and Physics, 13 (2013), pp. 2793–2825.
- [52] D. W. JORGENSEN, *Double dividend: environmental taxes and fiscal reform in the United States*, MIT Press, Cambridge, MA, 2013.
- [53] S. KATOCH, S. S. CHAUHAN, AND V. KUMAR, *A review on genetic algorithm: past, present, and future*, Multimedia Tools and Applications, 80 (2021), pp. 8091–8126.
- [54] D. W. KEITH, G. HOLMES, D. ST. ANGELO, AND K. HEIDEL, *A Process for Capturing CO₂ from the Atmosphere*, Joule, 2 (2018), pp. 1573–1594.
- [55] L. KEMP, C. XU, J. DEPLEDGE, K. L. EBI, G. GIBBINS, T. A. KOHLER, J. ROCKSTRÖM, M. SCHEFFER, H. J. SCHELLNHUBER, W. STEFFEN, AND T. M. LENTON, *Climate Endgame: Exploring catastrophic climate change scenarios*, Proceedings of the National Academy of Sciences, 119 (2022), p. e2108146119.
- [56] E. KRIEGLER, N. BAUER, A. POPP, F. HUMPERÖDER, M. LEIMBACH, J. STREFLER, L. BAUMSTARK, B. L. BODIRSKY, J. HILAIRE, D. KLEIN, I. MOURATIADOU, I. WEINDL, C. BERTRAM, J.-P. DIETRICH, G. LUDEKER, M. PEHL, R. PIETZCKER, F. PIONTEK, H. LOTZE-CAMPEN, A. BIEWALD, M. BONSCH, A. GIANNOUSAKIS, U. KREIDENWEIS, C. MÜLLER, S. ROLINSKI, A. SCHULTES, J. SCHWANITZ, M. STEVANOVIC, K. CALVIN, J. EMMERLING, S. FUJIMORI, AND O. EDENHOFER, *Fossil-fueled development (SSP5): An energy and resource intensive scenario for the 21st century*, Global Environmental Change, 42 (2017), pp. 297–315.
- [57] K. S. LACKNER, R. AINES, S. ATKINS, A. ATKISSON, S. BARRETT, M. BARTEAU, R. J. BRAUN, J. BROUWER, W. BROECKER, J. B. BROWNE, R. DARTON, N. DEICH, J. EDMONDS, P. EISENBERGER, P. S. FENNELL, P. FLYNN, T. FOX, S. J. FRIEDMANN, M. GERRARD, J. GIBBINS, C. VAN DER GIESEN, D. S. GOLDBERG, C. GRAVES, R. GUPTA, M. HANEMANN, D. KEITH, R. KLEIJN, G. J. KRAMER, T. KRUGER, M. MAZZOTTI, C. J. MEINRENKEN, G. T. R. PALMORE, A.-H. A. PARK, A. PUTNAM, V. RAO, G. H. RAU, S. RAYNER, B. E. RITTMANN, J. D. SACHS, D. SAREWITZ, P. SCHLOSSER, J. P. SEVERINGHAUS, E. B. STECHEL,

- A. STEINFELD, C. E. THOMAS, AND W. C. TURKENBURG, *The promise of negative emissions*, Science, 354 (2016), pp. 714–714.
- [58] K. S. LACKNER, S. BRENNAN, J. M. MATTER, A.-H. A. PARK, A. WRIGHT, AND B. VAN DER ZWAAN, *The urgency of the development of CO₂ capture from ambient air*, Proceedings of the National Academy of Sciences, 109 (2012), pp. 13156–13162.
- [59] F. LEHNER, C. DESER, N. MAHER, J. MAROTZKE, E. M. FISCHER, L. BRUNNER, R. KNUTTI, AND E. HAWKINS, *Partitioning climate projection uncertainty with multiple large ensembles and CMIP5/6*, Earth System Dynamics, 11 (2020), pp. 491–508.
- [60] D. LEMOINE AND I. RUDIK, *Managing Climate Change Under Uncertainty: Recursive Integrated Assessment at an Inflection Point*, Annual Review of Resource Economics, 9 (2017), pp. 117–142.
- [61] T. M. LENTON, H. HELD, E. KRIEGLER, J. W. HALL, W. LUCHT, S. RAHMSTORF, AND H. J. SCHELLNHUBER, *Tipping elements in the Earth's climate system*, Proceedings of the National Academy of Sciences, 105 (2008), pp. 1786–1793.
- [62] A. H. MACDOUGALL, *The Transient Response to Cumulative CO₂ Emissions: a Review*, Current Climate Change Reports, 2 (2016), pp. 39–47.
- [63] N. G. MANKIW, M. WEINZIERL, AND D. YAGAN, *Optimal Taxation in Theory and Practice*, Journal of Economic Perspectives, 23 (2009), pp. 147–174.
- [64] H. D. MATTHEWS, N. P. GILLETT, P. A. STOTT, AND K. ZICKFELD, *The proportionality of global warming to cumulative carbon emissions*, Nature, 459 (2009), pp. 829–832.
- [65] M. D. MCKAY, R. J. BECKMAN, AND W. J. CONOVER, *A Comparison of Three Methods for Selecting Values of Input Variables in the Analysis of Output from a Computer Code*, Technometrics, 21 (1979), p. 239.
- [66] MCKINSEY & COMPANY, *Pathways to a low-carbon economy: Version 2 of the global greenhouse gas abatement cost curve*, Stockholm, Sept. 2013.
- [67] F. MEIER AND C. P. TRAEGER, *SolACE - Solar Geoengineering in an Analytic Climate Economy*, Aug. 2022.
- [68] M. MEINSHAUSEN, N. MEINSHAUSEN, W. HARE, S. C. B. RAPER, K. FRIELE, R. KNUTTI, D. J. FRAME, AND M. R. ALLEN, *Greenhouse-gas emission targets for limiting global warming to 2 °C*, Nature, 458 (2009), pp. 1158–1162.
- [69] M. MEINSHAUSEN, Z. R. J. NICHOLLS, J. LEWIS, M. J. GIDDEN, E. VOGEL, M. FREUND, U. BEYERLE, C. GEISSNER, A. NAUELS, N. BAUER, J. G. CANADELL, J. S. DANIEL, A. JOHN, P. B. KRUMMEL, G. LUDERER, N. MEINSHAUSEN, S. A. MONTZKA, P. J. RAYNER, S. REIMANN, S. J. SMITH, M. VAN DEN BERG, G. J. M. VELDERS, M. K. VOLLMER, AND R. H. J. WANG, *The shared socio-economic pathway (SSP) greenhouse gas concentrations and their extensions to 2500*, Geoscientific Model Development, 13 (2020), pp. 3571–3605.

- [70] M. MITCHELL, *An introduction to genetic algorithms*, Complex adaptive systems, Cambridge, Mass., 7. print ed., 2001.
- [71] F. C. MOORE AND D. B. DIAZ, *Temperature impacts on economic growth warrant stringent mitigation policy*, Nature Climate Change, 5 (2015), pp. 127–131.
- [72] NATIONAL CENTER FOR ENERGY ECONOMICS, *Supplementary Material for the Regulatory Impact Analysis for the Supplemental Proposed Rulemaking, “Standards of Performance for New, Reconstructed, and Modified Sources and Emissions Guidelines for Existing Sources: Oil and Natural Gas Sector Climate Review”*, U.S. Environmental Protection Agency, Washington D.C., Sept. 2022.
- [73] NATIONAL RESEARCH COUNCIL, *Climate Intervention: Carbon Dioxide Removal and Reliable Sequestration*, National Academies Press, Washington, D.C., June 2015.
- [74] NEW YORK STATE ENERGY RESEARCH AND DEVELOPMENT AUTHORITY AND RESOURCES FOR THE FUTURE, *Estimating the cost of carbon: two approaches*, tech. rep., Oct. 2020.
- [75] R. G. NEWELL, W. A. PIZER, AND B. C. PREST, *A Discounting Rule for the Social Cost of Carbon*, Journal of the Association of Environmental and Resource Economists, 9 (2022), pp. 1017–1046.
- [76] W. D. NORDHAUS, *An Optimal Transition Path for Controlling Greenhouse Gases*, Science, 258 (1992), pp. 1315–1319.
- [77] ——, *Economic aspects of global warming in a post-Copenhagen environment*, Proceedings of the National Academy of Sciences, 107 (2010), pp. 11721–11726.
- [78] ——, *Revisiting the social cost of carbon*, Proceedings of the National Academy of Sciences, 114 (2017), pp. 1518–1523.
- [79] B. OBAMA, *The irreversible momentum of clean energy*, Science, 355 (2017), pp. 126–129.
- [80] R. S. PINDYCK, *Climate Change Policy: What Do the Models Tell Us?*, Journal of Economic Literature, 51 (2013), pp. 860–872.
- [81] C. PROISTOESCU AND G. WAGNER, *Uncertainties in Climate and Weather Extremes Increase the Cost of Carbon*, One Earth, 2 (2020), pp. 515–517.
- [82] F. P. RAMSEY, *A Mathematical Theory of Saving*, The Economic Journal, 38 (1928), p. 543.
- [83] K. RENNERT, F. ERRICKSON, B. C. PREST, L. RENNELS, R. G. NEWELL, W. PIZER, C. KINGDON, J. WINGENROTH, R. COOKE, B. PARTHUM, D. SMITH, K. CROMAR, D. DIAZ, F. C. MOORE, U. K. MÜLLER, R. J. PLEVIN, A. E. RAFTERY, H. ŠEVČÍKOVÁ, H. SHEETS, J. H. STOCK, T. TAN, M. WATSON, T. E. WONG, AND D. ANTHOFF, *Comprehensive Evidence Implies a Higher Social Cost of CO₂*, Nature, (2022).

- [84] K. RIAHI, C. BERTRAM, D. HUPPMANN, J. ROGELJ, V. BOSETTI, A.-M. CABARDOS, A. DEPPERMANN, L. DROUET, S. FRANK, O. FRICKO, S. FUJIMORI, M. HARMSEN, T. HASEGAWA, V. KREY, G. LUDEKER, L. PAROUSSOS, R. SCHAEFFER, M. WEITZEL, B. VAN DER ZWAAN, Z. VRONTISI, F. D. LONGA, J. DESPRÉS, F. FOSSE, K. FRAGKIADAKIS, M. GUSTI, F. HUMPERNÖDER, K. KERAMIDAS, P. KISHIMOTO, E. KRIEGLER, M. MEINSHAUSEN, L. P. NOGUEIRA, K. OSHIRO, A. POPP, P. R. R. ROCHEDO, G. ÜNLÜ, B. VAN RUIVEN, J. TAKAKURA, M. TAVONI, D. VAN VUREN, AND B. ZAKERI, *Cost and attainability of meeting stringent climate targets without overshoot*, Nature Climate Change, 11 (2021), pp. 1063–1069.
- [85] K. RIAHI, D. P. VAN VUREN, E. KRIEGLER, J. EDMONDS, B. C. O’NEILL, S. FUJIMORI, N. BAUER, K. CALVIN, R. DELLINK, O. FRICKO, W. LUTZ, A. POPP, J. C. CUARESMA, S. KC, M. LEIMBACH, L. JIANG, T. KRAM, S. RAO, J. EMMERLING, K. EBI, T. HASEGAWA, P. HAVLIK, F. HUMPERNÖDER, L. A. DA SILVA, S. SMITH, E. STEHFEST, V. BOSETTI, J. EOM, D. GERNAAT, T. MASUI, J. ROGELJ, J. STREFLER, L. DROUET, V. KREY, G. LUDEKER, M. HARMSEN, K. TAKAHASHI, L. BAUMSTARK, J. C. DOELMAN, M. KAINUMA, Z. KLIMONT, G. MARANGONI, H. LOTZE-CAMPEN, M. OBERSTEINER, A. TABEAU, AND M. TAVONI, *The Shared Socioeconomic Pathways and their energy, land use, and greenhouse gas emissions implications: An overview*, Global Environmental Change, 42 (2017), pp. 153–168.
- [86] R. G. RICHELS AND G. J. BLANFORD, *The value of technological advance in decarbonizing the U.S. economy*, Energy Economics, 30 (2008), pp. 2930–2946.
- [87] J. RISING, M. TEDESCO, F. PIONTEK, AND D. A. STAINFORTH, *The missing risks of climate change*, Nature, 610 (2022), pp. 643–651.
- [88] J. ROGELJ, A. POPP, K. V. CALVIN, G. LUDEKER, J. EMMERLING, D. GERNAAT, S. FUJIMORI, J. STREFLER, T. HASEGAWA, G. MARANGONI, V. KREY, E. KRIEGLER, K. RIAHI, D. P. VAN VUREN, J. DOELMAN, L. DROUET, J. EDMONDS, O. FRICKO, M. HARMSEN, P. HAVLÍK, F. HUMPERNÖDER, E. STEHFEST, AND M. TAVONI, *Scenarios towards limiting global mean temperature increase below 1.5 °C*, Nature Climate Change, 8 (2018), pp. 325–332.
- [89] S. K. ROSE, D. B. DIAZ, AND G. J. BLANFORD, *Understanding the Social Cost of Carbon: A Model Diagnostic and Inter-comparison Study*, Climate Change Economics, 08 (2017), p. 1750009.
- [90] T. S. SCHMIDT AND S. SEWERIN, *Technology as a driver of climate and energy politics*, Nature Energy, 2 (2017), p. 17084.
- [91] F. SCHROYEN AND K. O. AARBU, *Attitudes Towards Large Income Risk in Welfare States: An International Comparison*, Dec. 2017.
- [92] R. SOCOLOW, M. DESMOND, R. AINES, J. BLACKSTOCK, O. BOLLAND, T. KAARSBERG, N. LEWIS, M. MAZZOTTI, A. PFEFFER, K. SAWYER, ET AL., *Direct air capture of CO₂ with chemicals: a technology assessment for the aps panel on public affairs*, tech. rep., American Physical Society, 2011.

- [93] N. STERN, *The Structure of Economic Modeling of the Potential Impacts of Climate Change: Grafting Gross Underestimation of Risk onto Already Narrow Science Models*, Journal of Economic Literature, 51 (2013), pp. 838–859.
- [94] L. SUMMERS AND R. ZECKHAUSER, *Policymaking for posterity*, Journal of Risk and Uncertainty, 37 (2008), pp. 115–140.
- [95] J. TAKAKURA, S. FUJIMORI, N. HANASAKI, T. HASEGAWA, Y. HIRABAYASHI, Y. HONDA, T. IIZUMI, N. KUMANO, C. PARK, Z. SHEN, K. TAKAHASHI, M. TAMURA, M. TANOU, K. TSUCHIDA, H. YOKOKI, Q. ZHOU, T. OKI, AND Y. HIJOKA, *Dependence of economic impacts of climate change on anthropogenically directed pathways*, Nature Climate Change, 9 (2019), pp. 737–741.
- [96] M. V. THOMPSON AND J. T. RANDERSON, *Impulse response functions of terrestrial carbon cycle models: method and application*, Global Change Biology, 5 (1999), pp. 371–394.
- [97] R. TOL, *Safe policies in an uncertain climate: an application of FUND*, Global Environmental Change, 9 (1999), pp. 221–232.
- [98] UNITED NATIONS FRAMEWORK CONVENTION ON CLIMATE CHANGE, *Adoption of the Paris Agreement. I: Proposal by the President*, United Nations Office, Geneva, 2015.
- [99] UNIVERSITÄT HAMBURG AND CESIFO, M. D. BAUER, G. D. RUDEBUSCH, AND FEDERAL RESERVE BANK OF SAN FRANCISCO, *The Rising Cost of Climate Change: Evidence from the Bond Market*, Federal Reserve Bank of San Francisco, Working Paper Series, (2020), pp. 1–39.
- [100] D. P. VAN VUREN, E. STEHFEST, D. E. GERNAAT, J. C. DOELMAN, M. VAN DEN BERG, M. HARMSEN, H. S. DE BOER, L. F. BOUWMAN, V. DAILOGLOU, O. Y. EDELENBOSCH, B. GIROD, T. KRAM, L. LASSALETTA, P. L. LUCAS, H. VAN MEIJL, C. MÜLLER, B. J. VAN RUIJVEN, S. VAN DER SLUIS, AND A. TABEAU, *Energy, land-use and greenhouse gas emissions trajectories under a green growth paradigm*, Global Environmental Change, 42 (2017), pp. 237–250.
- [101] J. VON NEUMANN AND O. MORGENSTERN, *Theory of games and economic behavior*, Princeton University Press, 1947.
- [102] G. WAGNER, T. KÅBERGER, S. OLAI, M. OPPENHEIMER, K. RITTENHOUSE, AND T. STERNER, *Energy policy: Push renewables to spur carbon pricing*, Nature, 525 (2015), pp. 27–29.
- [103] P. WEIL, *Nonexpected Utility in Macroeconomics*, The Quarterly Journal of Economics, 105 (1990), p. 29.
- [104] M. L. WEITZMAN, *GHG Targets as Insurance Against Catastrophic Climate Damages*, Journal of Public Economic Theory, 14 (2012), pp. 221–244.
- [105] WORLD BANK, *State and Trends of Carbon Pricing 2021*, serial, World Bank, Washington, DC, May 2021.

Supplementary information for “Financial modeling of climate risk supports stringent mitigation action”

Adam Michael Bauer*

Cristian Proistosescu†

Gernot Wagner‡

Working Paper

February 7, 2023

1 “No free lunches” calibration

As a sensitivity test of our marginal abatement cost curve (MACC), we increased the cost of each mitigation option by one cost bracket, eliminating the zero-cost mitigation options (i.e., “free lunch” options) that the IPCC reports in their WGIII report. The resulting cost figure is in Figure 1.

2 “Infinite cost” calibration

As another sensitivity test of our marginal abatement cost curve (MACC), we cut out the < \$0 abatement potential reported by the IPCC WGIII data and fit a curve to the nonzero cost options. The resulting cost figure is in Figure 2. Note that this marginal abatement cost curve (MACC) results in costs that are lower than the “no free lunches” calibration. Hence, we do not present Climate Asset Pricing model – AR6 runs with this cost curve specified, as the results will be simple interpolations between the main specification results and the “no free lunches” results.

3 Effective TCRE calibration check

In Table 1 we compare the average warming levels using our effective TCRE approach and the weighted model averages presented by the IPCC in AR6.

*Department of Physics, University of Illinois at Urbana Champaign, Loomis Laboratory, Urbana, IL 61801 (corresponding author: adammb4@illinois.edu)

†Department of Atmospheric Sciences & Department of Geology, University of Illinois at Urbana Champaign, Urbana, IL 61801 (cristi@illinois.edu)

‡Columbia Business School, New York, NY 10027 (gwagner@columbia.edu)

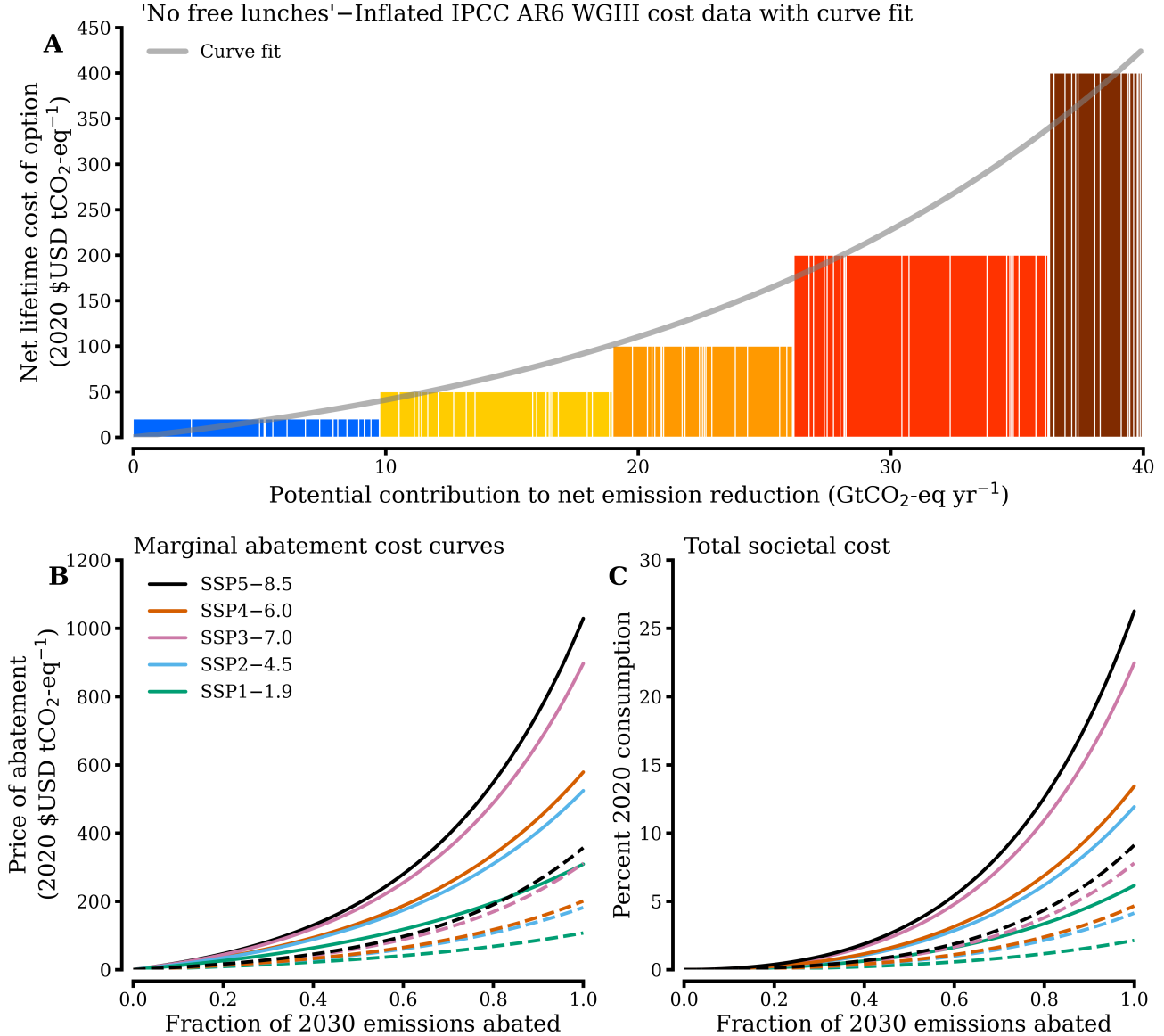


Figure 1: “No free lunches” cost calibration. Panel **A** shows the mitigation potential and cost for each methodology given by the IPCC using their WGIII data after adjusting for the “no free lunches” calibration. Blue bars represent the \$0 - \$20 range, yellow is \$20-\$50, orange is \$50-\$100, red is \$100-\$200, and maroon is our new cost bracket \$400. Our curve fit is in grey. Panel **B** shows the fitted marginal abatement cost curves and Panel **C** shows the total cost to society. In panels **B–C**, solid lines correspond to 2030, while dashed lines are cost curves in 2100, assuming an exogenous technological growth rate of 1.5% and no endogenous technological growth.

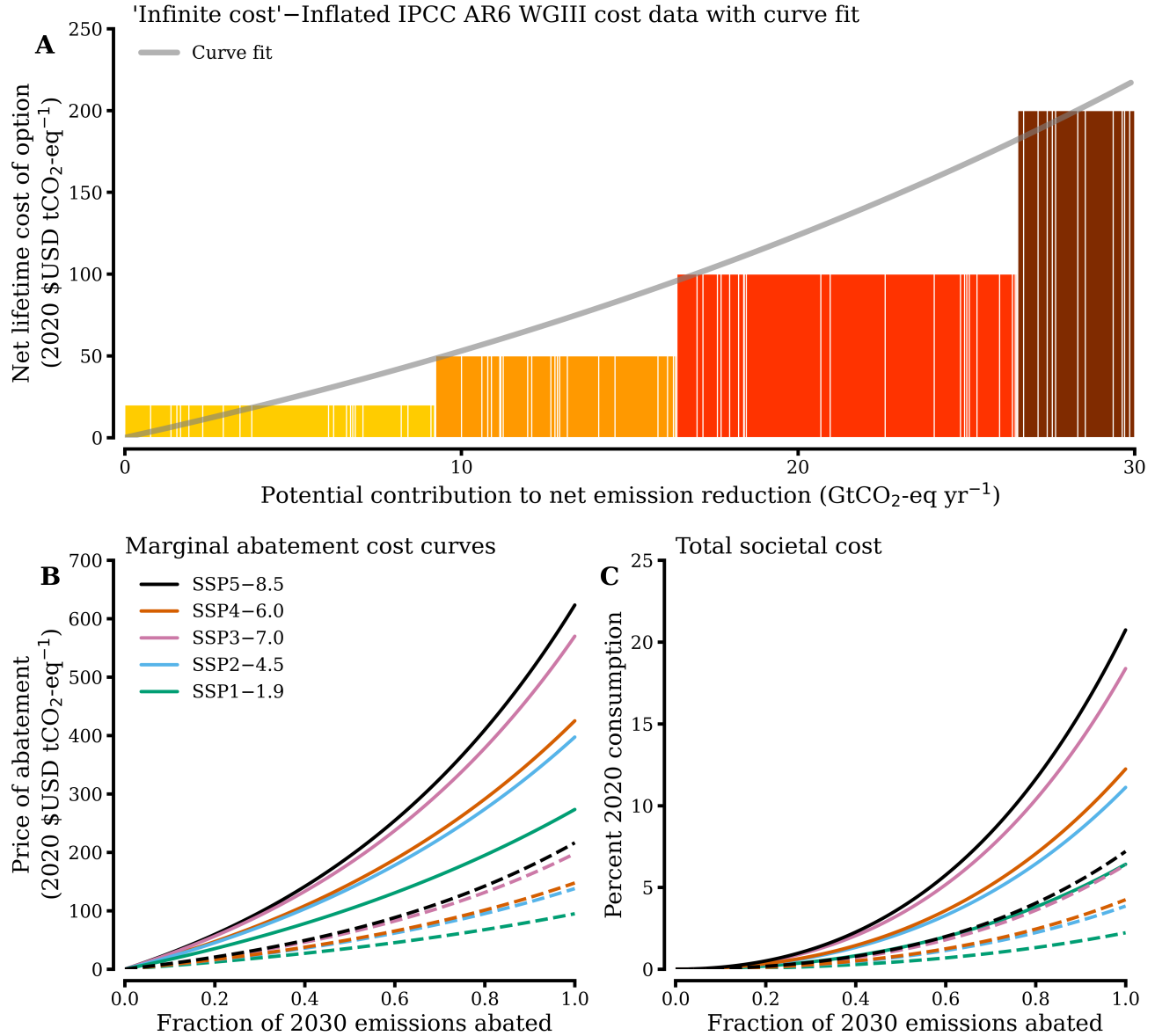


Figure 2: “Infinite cost” calibration. Panel **A** shows the mitigation potential and cost for each methodology given by the IPCC using their WGIII data after adjusting for the “infinite cost” calibration. Yellow bars are the \$0-\$20 range, orange is \$20-\$50, red is \$50-\$100, and maroon is \$100-\$200. Our curve fit is in grey. Panel **B** shows the fitted marginal abatement cost curves and Panel **C** shows the total cost to society. In panels **B–C**, solid lines correspond to 2030, while dashed lines are cost curves in 2100, assuming an exogenous technological growth rate of 1.5% and no endogenous technological growth.

Table 1: Effective TCRE comparison to AR6. Shown are the central estimate and the 5%-95% range of warming levels in three time periods, for three emissions baselines, using our effective TCRE approach and what is reported by the IPCC in their Table 4.5.

Time period	Effective TCRE range ($^{\circ}\text{C}$)	AR6 range ($^{\circ}\text{C}$)
SSP2–4.5		
Near-term: 2021–2040	1.5 (1.3 to 1.6)	1.5 (1.2 to 1.8)
Mid-term: 2041–2060	1.9 (1.5 to 2.4)	2.0 (1.6 to 2.5)
Long-term: 2081–2100	2.6 (1.7 to 3.5)	2.7 (2.1 to 3.5)
SSP3–7.0		
Near-term: 2021–2040	1.5 (1.3 to 1.7)	1.5 (1.2 to 1.8)
Mid-term: 2041–2060	2.1 (1.6 to 2.7)	2.1 (1.7 to 2.6)
Long-term: 2081–2100	3.6 (2.1 to 5.1)	3.6 (2.8 to 4.6)
SSP5–8.5		
Near-term: 2021–2040	1.5 (1.3 to 1.7)	1.6 (1.3 to 1.9)
Mid-term: 2041–2060	2.3 (1.6 to 2.9)	2.4 (1.9 to 3.0)
Long-term: 2081–2100	4.6 (2.4 to 6.8)	4.4 (3.3 to 5.7)

4 Supporting figures: Regression analysis

Here we show the supporting figures for the variance attribution we carried out in the main paper. Figure 3 is the regression of CO₂ prices against each parameter value. Figures 4, 5, and 6 are as Figure 3 but for global mean surface temperature change, CO₂ concentrations, and economic damages, respectively.

5 Impact of Epstein-Zin risk aversion on prices

Shown in Figure 7 is the influence of changing the Epstein-Zin risk aversion parameter, ψ , on CO₂ prices. Some near-term differences are seen, but overall, the value of ψ has very little influence on the price of CO₂.

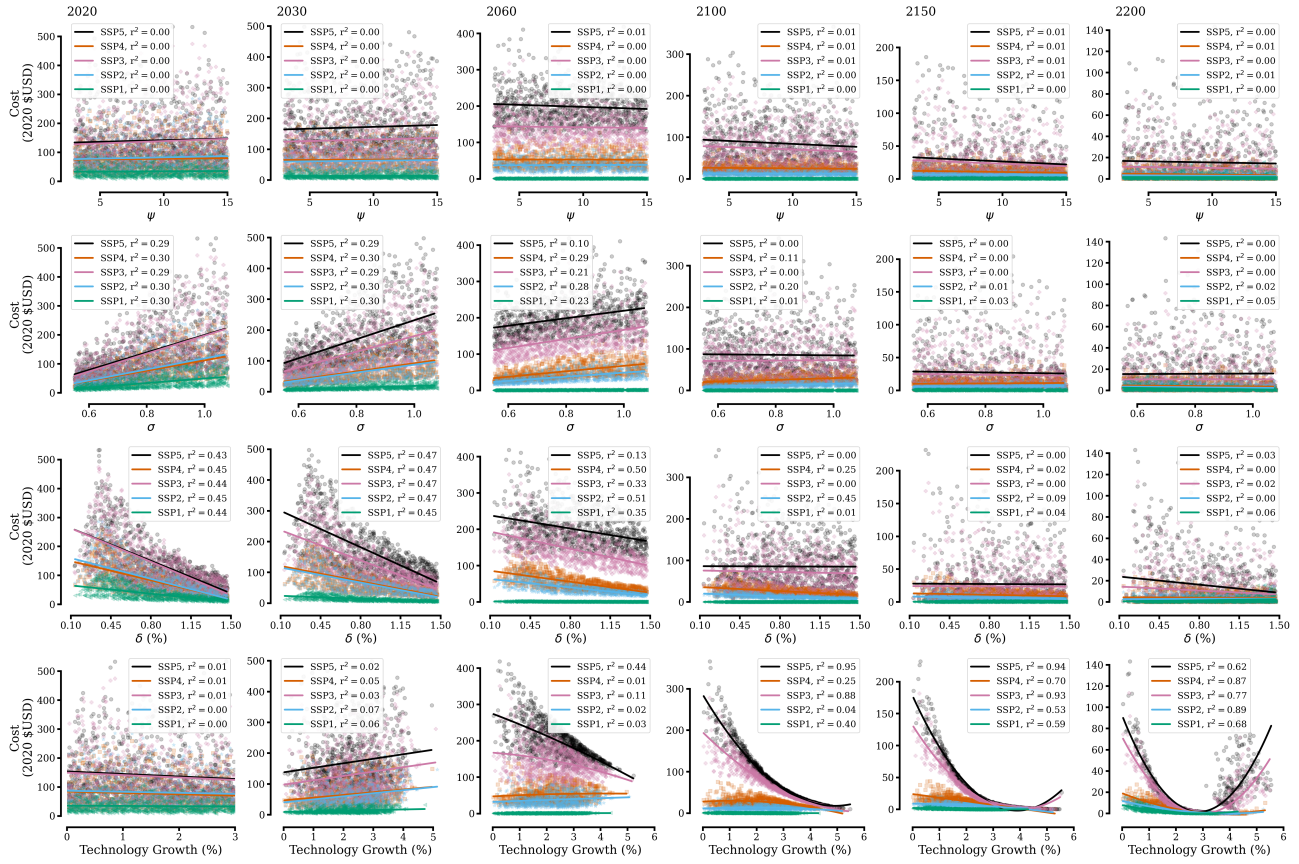


Figure 3: Cost of carbon regression plots. In each row, we plot the regression of each parameter against carbon costs in that period. r^2 values are given for each regression in the legend of each panel.

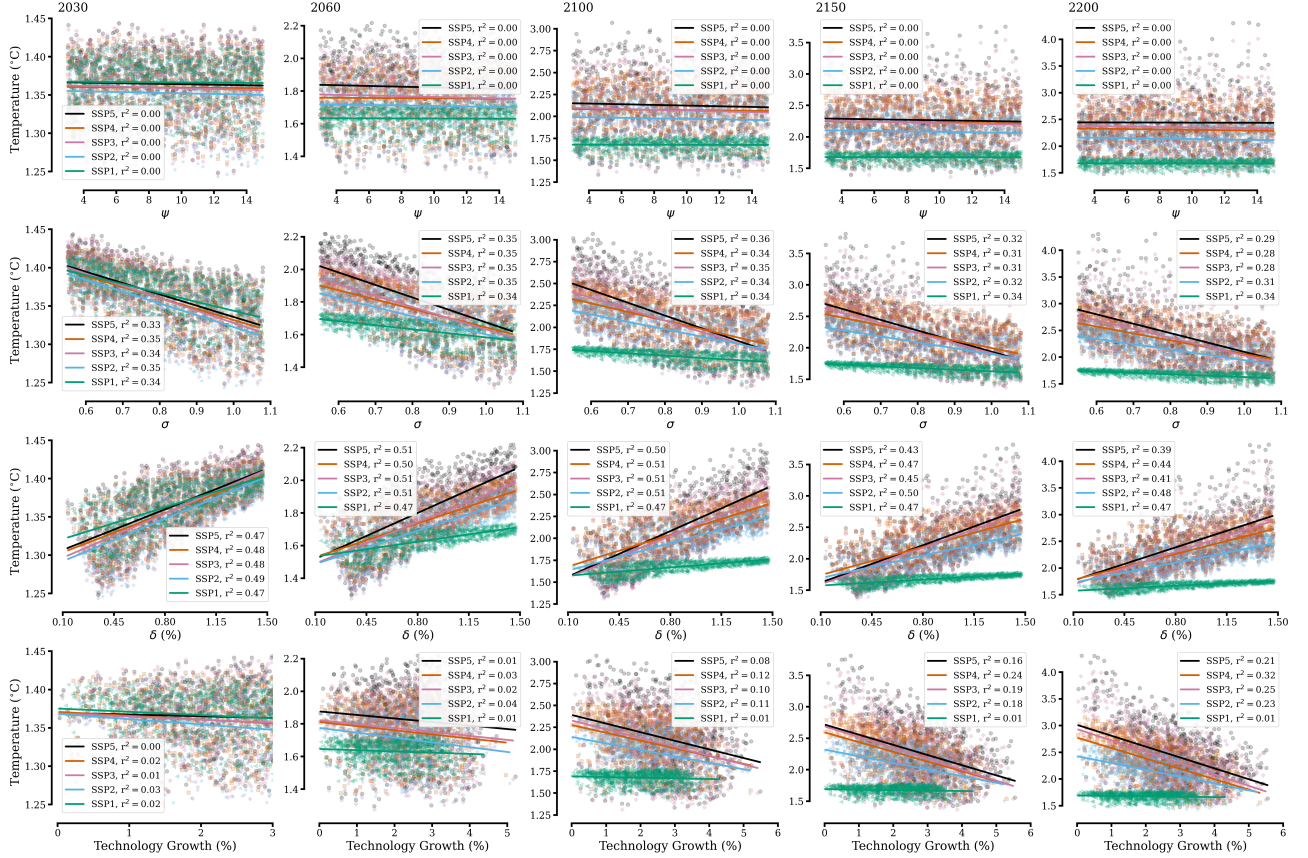


Figure 4: Temperature regression plots. In each row, we plot the regression of each parameter against temperature in that period. r^2 values are given for each regression in the legend of each panel.

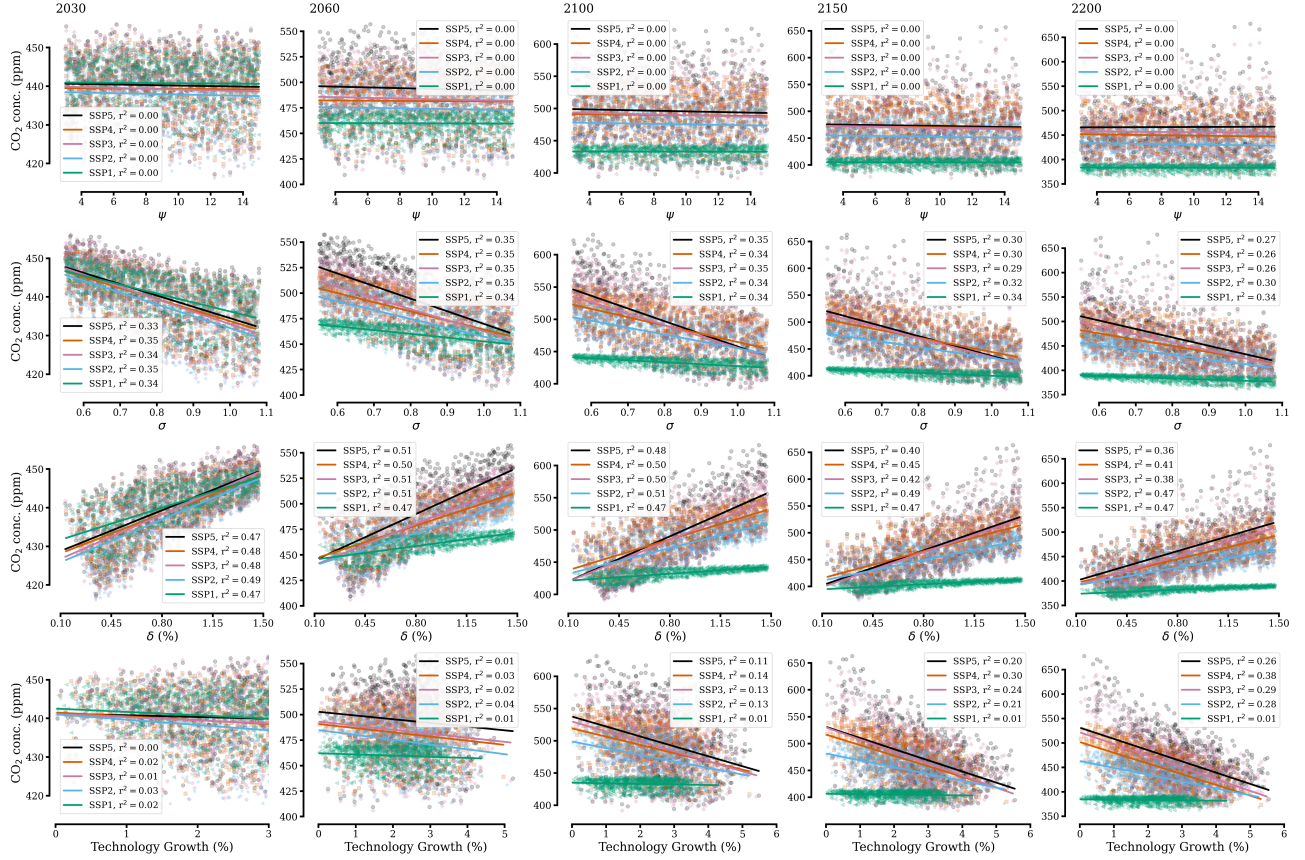


Figure 5: CO₂ concentrations regression plots. In each row, we plot the regression of each parameter against CO₂ concentrations in that period. r^2 values are given for each regression in the legend of each panel.

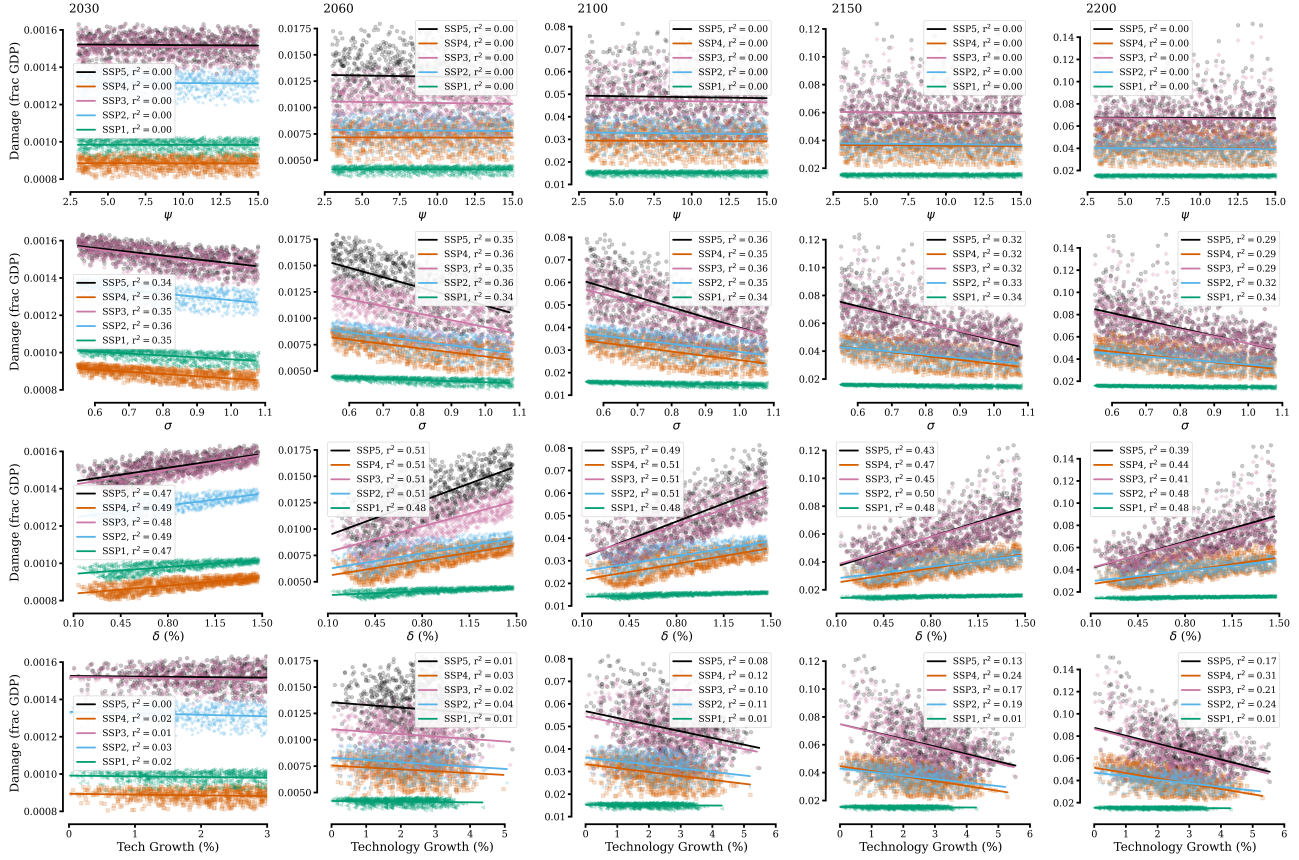


Figure 6: Economic damages regression plots. In each row, we plot the regression of each parameter against economic damages in that period. r^2 values are given for each regression in the legend of each panel.

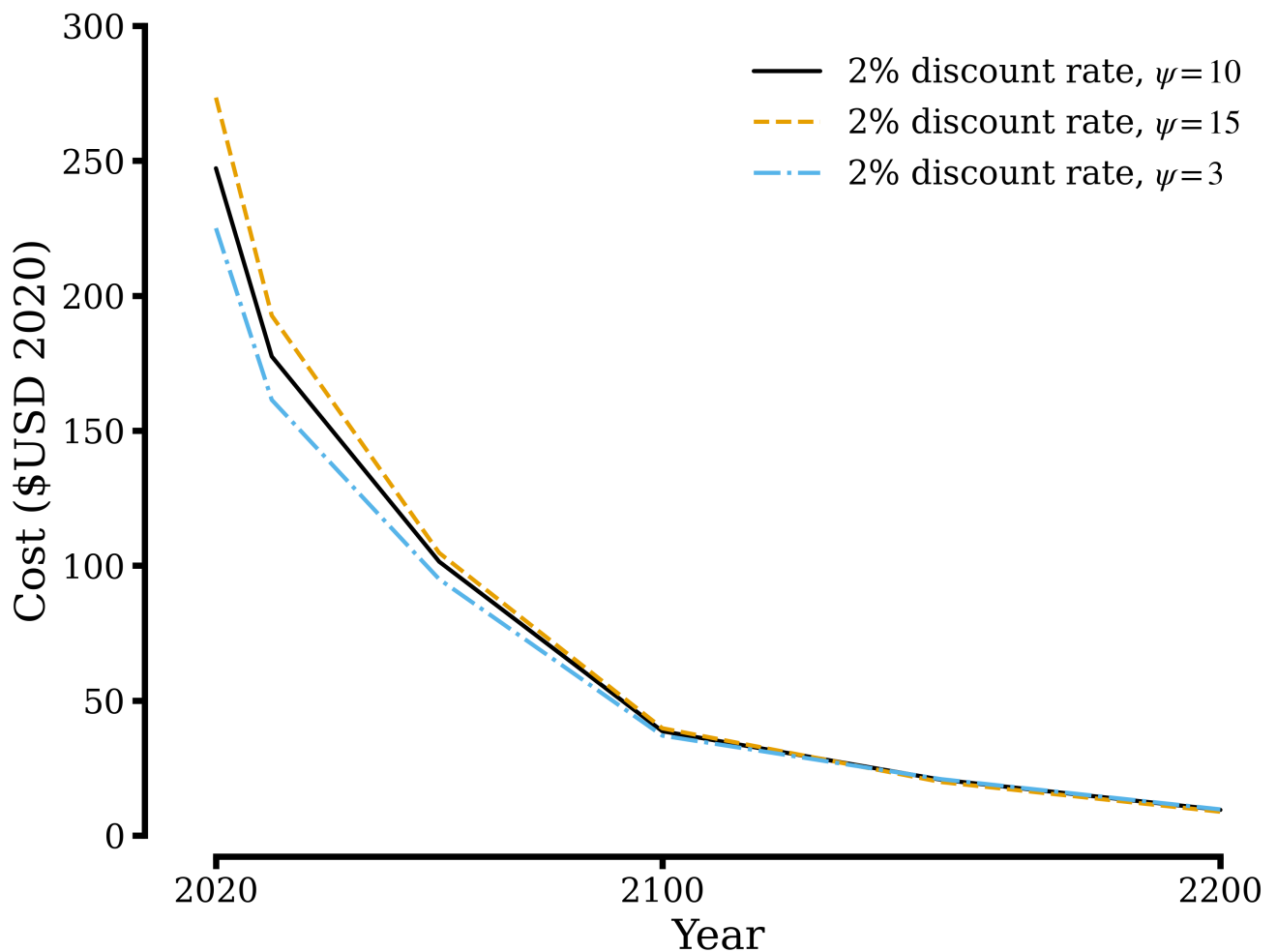


Figure 7: Risk aversion impact on price. Shown is the resulting price path for different choices of risk aversion, holding all other model inputs constant in our preferred calibration.